C.P. No. 735

C.P. No. 735

MINISTRY OF AVIATION

AERONAUTICAL RESEARCH COUNCIL

CURRENT PAPERS

8ft x 6ft Tunnel Tests on a Model of the De Havilland "Blue Streak" at Mach Numbers of 0.80 to 1.25

by

A. L. Courtney, B Sc.

LONDON: HER MAJESTY'S STATIONERY OFFICE

1964

EIGHT SHILLINGS NET

U.D.C. No. 533.665:533.6.011.35:533.6.013.1:Blue Streak

C.P. No.735

April, 1959

8 FT X 6 FT TUNNEL TESTS ON A MODEL OF THE DE HAVILLAND "BLUE STREAK" AT MACH NUMBERS OF 0.80 TO 1.25

by

A.L. Courtney, B.Sc.

SUMMARY

Six-component force and moment measurements have been made on a fully representative model of the De Havilland "Blue Streak" at Mach numbers of 0.80 to 1.25, body incidences up to 15° and roll angles up to 90°, to check the static stability characteristics in the transonic speed range.

With fins off the results are free from serious irregularities and the pitching moment is approximately linear with body incidence (θ) about the full-scale centre-of-gravity position. With fins on there is some non-linearity in pitch, particularly at subsonic speeds.

The values of $dC_m/d\theta$ at zero roll angle are greater than was expected from simple cone-cylinder tests, the difference amounting to about 28% at M=1 about the full-scale centre-of-gravity position. Component tests show that the increase is entirely attributable to the various external fitments (stringers, fuel pipes, nose blister, rear pods and rear step) all of which increase $dC_m/d\theta$.

Replaces R.A.E. Tech. Note No. Aero 2610 - A.R.C. 21756.

The results of the R.A.E. Bedford 8 ft and 3 ft tunnel tests, with which the present results are compared in Section 4.4 and elsewhere, have now been published and the references are as follows:-

E. Huntley	Wind tunnel measurements of normal force and pitching moment at a Mach number of 2.00 on a 1 : 30 scale model of Blue Streak. A.R.C. C.P. 732, May 1959.
G.F. Moss and D. Isaacs	8 ft x 8 ft tunnel tests on a model of the De Havilland 'Blue Streak'. A.R.C. C.P. 734, July 1961.

LIST OF CONTENTS

LIST OF TABLES

LIST OF ILLUSTRATIONS

LIST OF ILLUSTRATIONS (CONT'D)

1 INTRODUCTION

Tests have been made on a model of the De Havilland "Blue Streak" missile in the R.A.E. 8 ft x 6 ft Transonic Tunnel, as a check on the static stability characteristics at Mach numbers between 0.8 and 1.25. Measurements were made of normal force, pitching moment, side force, yawing moment, rolling moment and axial force at body incidences of up to 15° and roll angles up to 90°, with fins on and off. Three head shapes were tested and the effects of various components such as external stringers, fuel pipes, nose blister, rear pods and a rear step (Fig.1) were investigated at zero roll angle.

Selected results are presented graphically to illustrate the main trends and the effects of the various modifications. Comparisons are made with the results of tests on the same model in the 3 ft x 3 ft and 8 ft x 8 ft tunnels at R.A.E. Bedford, and on a simplified cone-cylinder model ("Model 80") in the 3 ft x 3 ft tunnel.

2 DESCRIPTION OF MODEL AND TESTS

2.1 Model details

The model was constructed by De Havilland Propellers Ltd. in aluminium alloy and reproduced the external characteristics of the full-scale missile in some detail. Drawings are given in Figs.1 and 2 and photographs in Fig.3.

The model consisted basically of a cylinder 4 inches in diameter (D) and 19.5 inches (4.88D) long to which could be attached the three heads A, B and C and the various external fitments. The junction of the cylinder and the nose cone is referred to as the shoulder.

Head shapes. These are shown in Fig.2. The standard head A was made up of a frustrum of a 19.4° included-angle cone with a relatively bluff nose-cap having a radius of 0.544D. What would otherwise have been an abrupt junction between the nose-cap and the cone was faired by a corner radius of 0.06D. The overall length of the model with head A was 25.5 inches (6.38D). Head C was of similar type, with the same cone angle, but was 0.42D shorter and had a nose-cap radius of 0.495D. Head B consisted of head A up to the forward ends of the stringers (Fig.1) but with the bluff nose-cap of head A replaced by a 30.2° included-angle cone and a nose radius of 0.10D which faired tangentially into the cone, increasing the length by 0.60D.

Rear step. There was a step 2.5 inches from the rear of the cylinder at which the diameter was reduced from 4.0 inches to 3.6 inches (Fig.1). An annular sleeve was provided enabling this step to be filled in for some of the tests.

Stringers. In the basic configuration, fore-and-aft surface stringers were represented on the rear half of the cylinder ahead of the step, and on the nose cones up to 1 inch from the front of head A. Around the cylinder there were 48 stringers 0.05 inch high and 0.06 inch wide, and around the nose-cones there were 60 stringers 0.03 inch high and 0.05 inch wide. For some of the tests removal of the stringers on the nose cone was simulated by filling the spaces between them with Araldite to give a smooth surface. This condition is referred to briefly as "stringers off" although the nose-cone stringers were faired over rather than removed, and those on the cylinder were left untouched.

Rear pods. Two removable pods were fitted at the rear of the model on top and bottom surfaces, as sketched in Fig.1. These were roughly cylindrical in shape with a conical front fairing, and were solid.

A nose blister was fitted just ahead of the shoulder, with a nose shape similar to that of a high-speed aircraft canopy but with a 0.2 inch step towards the rear (Fig.1). This blister was also removable.

External pipes. Three removable pipes were fitted as shown in Fig.1. On the port side there was a short length of circular pipe on the rear part of the body at $41\frac{1}{4}^{\circ}$ above the horizontal, and a long circular pipe extending from ahead of the shoulder to ahead of the rear step at $41\frac{1}{4}^{\circ}$ below the horizontal. These pipes were respectively 0.08 inch and 0.10 inch in diameter, with centres 0.12 inch and 0.19 inch above the body surface. On the starboard side there was a larger pipe at $26\frac{1}{2}^{\circ}$ below the horizontal, extending from ahead of the shoulder to behind the rear step, and with cross-section as shown in Fig.1. The overall dimensions of this pipe were 0.28 inch wide by 0.16 inch high and it was mounted 0.08 inch above the body surface.

Fins. Four stub fins could be attached to the rear of the model, inclined at 45° to the principal planes. These had a root chord of 4.34 inches and a nett semispan of 1.24 inches and were of double-wedge section with thicknesses as shown in Fig.1.

In addition to these removable items there was a small fixed blister mounted on top of the body $4\frac{1}{2}$ inches ahead of the rear step, as shown in Fig.1.

The model was mounted on a 6-component internal strain-gauge balance and attached to the tunnel incidence strut by a central sting, Fig.3. The sting diameter was 1.57 inches at the base of the model, and the sting taper (included angle) was 2.2° over the first 2.7 inches behind the model, 4.7° for the next 10 inches and 17° for the next 5 inches. The annular space around the sting at the base of the model was filled, to within about 0.1 inch of the model internal diameter, by a base plate attached to the sting, Fig.3, minimizing secondary flows within the hollow model. The pressure inside the model, i.e. the effective "base" pressure, was measured by a pair of pressure tubes above and below the sting.

The tests were begun before the sting rolling gear was installed in the tunnel, and variation of model roll angle was therefore effected by rolling the model relative to the fixed sting and balance. Provision was made in the model for roll angles of 0, $22\frac{1}{2}$, 45, $67\frac{1}{2}$ and 90 degrees.

2.2 Description of tests

Most of the tests were made at Mach number intervals of 0.1 in the range M=0.8 to M=1.2, with additional measurements at 0.05 intervals in some cases. The body incidences tested were generally -3, -2, -1, 0, 1, 2, 3, 5, 7, 9, 12 and 15 degrees. The tests were done at constant roll angle and Mach number, varying incidence. The mean test Reynolds number was 1.94×10^6 per foot, giving a Reynolds number of 0.65×10^6 based on model diameter or 4.1×10^6 based on model length (head A). Measurements were made of normal force, pitching moment, side force, yawing moment, rolling moment and axial force, relative to axes fixed in the sting (axis and force conventions are discussed later). The static pressures at orifices in the roof and one wall were also measured to give some indication of the passage of the bow shock and expansion system down the tunnel.

The cases tested, and their identification numbers, were as follows:-

TABLE 1

Configurations tested

Case	Head	Roll	Stringers	Rear pods	Nose blister	Pipes	Fins	Step	Fig.
1	A	0	On	On	On	On	Off	Present	5
2	A	$22\frac{1}{2}^{o}$	Off	On	On	On	Off	Present	16
3	A	45^{o}	On	On	On	On	Off	Present	16
4	A	$67\frac{1}{2}^{o}$	Off	On	On	On	Off	Present	16
5	A	90^{o}	On	On	On	On	Off	Present	16
6	A	0	Off	On	On	On	On	Present	17
7	A	45^{o}	Off	On	On	On	On	Present	17
8	A	90^{o}	Off	On	On	On	On	Present	17
9	A	0	Off	On	On	On	Off	Present	6
10	B	0	On	On	On	On	Off	Present	5
11	B	0	Off	On	On	On	Off	Present	-
12	C	0	Off	On	On	On	Off	Present	5
13	A	0	On	Off	On	On	Off	Present	7
14	A	0	Off	Off	On	On	Off	Present	7
15	A	0	On	On	Off	On	Off	Present	-
16	A	0	Off	On	On	Off	Off	Present	6
17	A	0	Off	On	On	On	Off	Filled	7
18	A	0	Off	Off	On	On	Off	Filled	7

In the table the items primarily under investigation in each test are underlined.

The tests were performed in three stages (this accounts for the apparently arbitrary variation of stringer configuration in table 1). In February 1957 the basic model without fins was tested at roll angles of 0, 45° and 90°, and the effects of head B, the nose blister and the rear pods were examined (cases 1, 3, 5, 10, 13, 15). It was then decided to investigate the effects of fairing over the front stringers, and tests with this done were made in April 1957. The additional head C was tested at the same time and further roll angles of $22\frac{1}{2}^{o}$ and $67\frac{1}{2}^{o}$ were included (cases 2, 4, 9, 11, 12). The effects of the fins (6, 7, 8) and pipes (16) were also investigated. Finally, tests were made in July 1957 to investigate the effects of filling-in the rear step (cases 14, 17, 18).

3 REDUCTION, ACCURACY AND PRESENTATION OF RESULTS

3.1 Axes and definitions

As noted above, the model was rolled by rotating it relative to the sting and balance. The measured forces were therefore obtained about axes which moved with the model in pitch but did not rotate with it in roll, and this axis system has been retained in the final presentation of results. The unrolled model condition is as shown in Fig.1, with the rear pods in the vertical plane and the nose blister uppermost. A sketch is given in Fig.4, and it will be seen that following standard 8 ft x 6 ft Tunnel practice the normal force Z is regarded as positive downward and the axial force X as positive forward. In the figures the normal-force and axial-force coefficients are given as $(-C_Z)$ and $(-C_X)$, i.e. in the usual lift and drag senses.

The incidence θ referred to throughout the text and figures is the body incidence measured in the fixed (vertical) XZ-plane, as shown in Fig.4.

The force coefficients are based on the model frontal area $\pi D^2/4$ and the moment coefficients on $\pi D^3/4$. The centre for pitching and yawing moments is 2.16D behind the shoulder (Fig.2) for all cases.

3.2 Wall corrections

No corrections have been applied for wall constraint on Mach number and incidence, the effects of which are thought to be small. The model blockage ratio (frontal area divided by tunnel cross-sectional area) has the relatively low value of 0.18%. So far as shock reflections are concerned, static pressure readings at the tunnel walls and at the base of the model suggest that the reflected nose shock and expansion system cleared the base of the model by about M=1.15. Below about M=1.05 any reflected waves should be fairly weak. Between these speeds some interference from reflected waves is possible but the effects of this on the measured forces are not known. The effects are not thought to be large, however, since as will be seen below good agreement is obtained, after allowance for model differences, with the "Model 80" cone-cylinder tests in which the ratio of model length to working-section height was one-and-a-half times as great.

3.3 Accuracy

Neglecting a few points which were obviously either wrongly recorded or were recorded before steady conditions had been reached, the accuracy of the final coefficients, as indicated by the scatter of the experimental results, is as follows:-

C_X	±0.02	(4% of max. recorded value)
C_Y	±0.01	(5% " " ")
C_Z	±0.01	(1% " " ")
C_ℓ	±0.005	(13% " " ")
C_m	±0.025	(1% " " ")
C_n	±0.025	(10% " " ")

The inaccuracy in C_X is due largely to the temperature drift noted below (para 3.4). The inaccuracies of the other components are higher than the usual 8 ft x 6 ft Tunnel figure of ½% of the maximum recorded value. The reason for this is that, in the interests of speed, the model was built around an existing balance designed to measure considerably high loads than those actually experienced, and the 1% inaccuracies in C_Z and C_m are no higher than expected in view of this. The higher percentage inaccuracies in C_Y, C_ℓ and C_n are due simply to the fact that throughout the tests these quantities remained small.

3.4 Presentation

A selection of the measured coefficients is given graphically in Figs.5 to 22 as follows:-

Figs.5 to 15 deal with normal force and pitching moment at zero roll angle. Of these, Figs.5 to 10 represent direct measurements of the effects of head shape, stringers, nose blister, pipes, pods and rear step, with fins off. Because of the number of fittings involved it was not possible to test all combinations of them in order to determine mutual interferences; instead

measurements were made of the effect of removing each part in turn with the others all present. Exceptions to this are that the effects of the pipes and the rear step were measured with the forward stringers already faired over, and the effects of the pods and the rear step were determined together as well as separately in view of the possibility of large mutual interference. So far as the other items are concerned there is no reason to expect large interferences. On this assumption Figs.11 and 12 have been derived from the measured results, to illustrate the effects on normal-force and pitching-moment slopes and aerodynamic centre position of progressively stripping the model of external fittings, to give finally a derived "clean" condition. These derived results for the clean condition can then be compared with some earlier results on simple cone-cylinders (Model 80, described in para.4.3 below). The same assumption is also made in Figs.13 to 15 comparing the present results with results for the same model in other tunnels. The actual or adjusted condition of the model is given in each figure, together with a note of any adjustments that have been made to reduce the results to a common condition.

Figs.16 to 18 and Fig.21 show the effects on normal force and pitching moment of rolling the model by up to 90°, with fins on and off. For these tests the model was in the basic Blue Streak condition with all external fitments present. No tests were made on the effect of removing external fitments with the model rolled. Figs.19 and 20 illustrate a few trends in the side force, yawing moment and rolling moment behaviour; a fuller presentation is not given in the figures since these forces and moments are generally small compared with normal force and pitching moment.

Finally, Fig.22 shows some typical variations of axial force with Mach number at zero incidence. Only a limited number of axial-force results are shown because the balance used was of an early type having a relatively large drift of axial force reading with temperature, due to thermal stresses. Since the measurement of drag was not an important test requirement it was not considered worth while to spend the time required to allow for this drift in all cases, particularly in view of the scatter remaining after all allowances had been made (para.3.3). In the value of $(-C_X)_{nett}$ the measured base pressure is replaced by the free-stream static pressure. The base area used for this purpose is that with the rear step present (D = 3.6 inches).

In connection with the results for the model in the rolled condition, it should perhaps be noted that the external pipes and the nose blister are not symmetrical with respect to the model principal planes, so that the characteristics for roll angles between 90° and 360° may differ somewhat from those measured in the first quadrant. The chief reason for not covering the full 360° was that at the time of the tests, the object of rolling the model was simply to check that induced roll and cross-coupling effects on the rear pods and fins were not unduly large, and for this purpose 90° of roll sufficed. A few results have been obtained for roll angles up to 360° in the 8 ft × 8 ft Tunnel, Bedford, and these are referred to in para.4.5 below.

4 NORMAL-FORCE AND PITCHING MOMENT RESULTS

4.1 Basic configuration at zero roll angle, fins off

Plots of $(-C_Z)$ and C_m against incidence for different Mach numbers are given in Fig.5 for the basic configuration without fins. From these, and

from Figs.6 and 7 giving similar results for other configurations, it can be seen that the curves are free from marked irregularities within the test incidence range of -5° to 15°. The normal force is of course non-linear with incidence due to cross-flow effects on the body, but the pitching moment varies more or less linearly with incidence about the chosen axis position 2.16D behind the shoulder, which corresponds approximately to the full-scale centre of gravity position for this speed range.

The values of $(-dC_Z/d\theta)$ and $dC_m/d\theta$ at zero incidence, and the aerodynamic centre position as given by the ratio of the two, are plotted against Mach number in Figs.11 and 12. At M=1.0, $dC_m/d\theta$ is 0.131 and the aerodynamic centre is 0.8D ahead of the shoulder. Compared with the results of the early Model 80 cone-cylinder tests*, which are also shown on Figs.11 and 12, $dC_m/d\theta$ at the chosen axis position is 28% greater at M=1, and the aerodynamic centre is about 0.5D further forward. One object of some of the further tests was to investigate possible sources of this increased instability of the fully representative Blue Streak model compared with Model 80. To avoid misunderstanding it should perhaps be pointed out that there is no requirement for positive static stability on this model; on the full-scale missile artificial stability is provided by swivelling rocket exits at the rear.

4.2 Effect of various modifications at zero roll angle

4.2.1 Head shape

The change from head A to the more conical head B has little effect on C_Z and C_m despite the increase in length of 0.6D. For the shorter head C, however, there are significant differences, particularly at Mach numbers of 0.8 and 0.9 where $dC_m/d\theta$ at zero incidence is reduced by between 10% and 15%, Fig.5. At supersonic speeds there is little effect on $dC_m/d\theta$ but there is a small increase in $(-dC_Z/d\theta)$.

4.2.2 Stringers

The effect of fairing over the forward stringers is illustrated for one case in Fig.6. Similar effects occur for other cases, e.g. with head B in place of head A and with rear pods off instead of on. The stringers are responsible for increases in both normal-force slope and pitching-moment slope throughout the test Mach number range. At zero incidence the effects are greatest near M=1.0, where $(-dC_Z/d\theta)$ is increased by 0.004 (10%) and $dC_m/d\theta$ by 0.004 (3%), and the aerodynamic centre is moved rearward by 0.25D, as illustrated in Figs.11 and 12. At this Mach number the centre of pressure of the added normal force is about one diameter behind the shoulder.

4.2.3 Pipes

These also increase the normal-force and pitching-moment slopes, Fig.6. At M=1.0 and zero incidence $(-dC_Z/d\theta)$ is increased by 0.003 (3%) and $dC_m/d\theta$ by 0.007 (6%), and these increments are about the same throughout the Mach number range, as illustrated in Fig.12. The pipes give a rearward aerodynamic centre shift of about 0.1D and the centre of pressure of the added normal force is about two diameters behind the shoulder.

---

* A description of Model 80 is given in para 4.3 below; see also Fig.2.

4.2.4 Nose blister

The effect of the nose blister is not large and curves against incidence are therefore not presented. As indicated in Fig.12 the blister increases $(-dC_Z/d\theta)$ at zero incidence by about 0.001, and decreases $dC_m/d\theta$ by about 0.001 at supersonic speeds.

4.2.5 Combined effect of stringers, pipes and nose blister

The combined effect of these apparently minor external fittings is quite large. At M=1 and zero incidence, for instance, they increase the normal-force slope by about 20% and the pitching-moment slope by about 8%, and move the aerodynamic centre rearward by about 0.4D. Compared with the simple Model 80 results, Figs.11 and 12 indicate that allowance for these items would account for about 35% of the discrepancy in $dC_m/d\theta$ at M=1 noted in para 4.1; however, the discrepancy in aerodynamic centre position would be increased, from 0.5D to 0.9D, because of the accompanying change in normal-force slope.

4.2.6 Effect of rear step and pods

The remaining significant external differences between Blue Streak and Model 80 are the rear step and pods, and the effects of these will be considered together in view of the mutual interference between them.

Fig.7(a) gives the normal-force and pitching-moment results with and without the rear step, with pods on. Fig.7(b) gives the corresponding results with pods off. Figs.8 and 9 show the effects of pods and step respectively on the normal-force and pitching-moment slopes at zero incidence, including results from the 3 ft x 3 ft Tunnel, Bedford on the present model and on Model 80.

The results show that at transonic speeds both the pods and the rear step decrease the normal-force slope and increase the pitching-moment slope, i.e. they produce a loss of lift acting near the rear of the model. In the case of the step this is as would be expected in view of the effective boat-tailing of the flow behind the step at these Mach numbers, and the maximum decrease in the measured normal-force slope of 0.006 at M=0.9, Fig.9, agrees well with the estimated value of 0.007 from slender-body theory assuming re-attachment at the base of the model. At higher Mach numbers experience shows that re-attachment fails to occur and this probably accounts for the much smaller effect of the step beyond M=1. In the case of the pods the reason for the loss of lift is not known.

Figs.8 and 9 show that there is considerable interference between the pods and the step. At M=1, for instance, the increase in pitching-moment slope due to the pods is 0.011 with the step filled but only 0.004 with the step present. Likewise the increase due to the step is 0.014 with pods off but only 0.005 with pods on. Fig.10 shows the rearward aerodynamic centre movement due to filling-in the step. With pods off there is a maximum shift of 0.7D compared with only about 0.2D with pods on.

The combined effect of pods and step on the zero incidence normal-force and pitching-moment slopes and aerodynamic centre position can be seen from Figs.11 and 12. They are responsible for an increase of pitching-moment slope of 0.019 (about 20%) at Mach numbers of 0.8 to 1.0, with a smaller effect at M=1.1, 1.2. The combined forward aerodynamic centre movement amounts to 0.75D at Mach numbers of 0.8 to 1.0, falling to 0.35D at M=1.2.

4.3 Comparison with Model 80 results at zero roll

Figs.11 and 12 enable the present results to be compared with unpublished tests made on Model 80 in the 3 ft x 3 ft Tunnel Bedford. This model consisted of a plain cylinder to which heads of different cone-angles and spherical nose radii were fitted. Of the shapes tested, head B of the Model 80 series most nearly represents the basic head A of the present tests. The shapes are compared in Fig.2 and it can be seen that the chief difference is in the nose cap, which has a smaller radius on Model 80 and fairs tangentially into the nose cone. Also, the cylindrical body is 0.2D shorter on Model 80.

As noted earlier Figs.11 and 12 show quite large differences in zero-incidence pitching-moment slope and aerodynamic centre between Model 80 and the basic Blue Streak configuration (stringers, pipes, pods and nose blister on, step unfaired and fins off). The differences are largest near M=1, where Blue Streak has a pitching-moment slope 0.029 (28%) greater than Model 80, an aerodynamic centre position 0.52D further forward and a somewhat higher normal-force slope. In the figures, intermediate curves are given showing the effect of progressively removing or fairing over the various external fitments on Blue Streak, to give finally a derived "clean" condition. As noted in para 3.4, it was necessary to assume that the effects of certain items were additive without additional interferences in deriving Figs.11 and 12. The nearest approach to a fully clean condition in the tests was Case 18 of table 1, for which the stringers and rear pods were removed and the step was filled, but the nose blister and the pipes remained and had to be allowed for on the basis of measurements made at other model conditions. Figs.11 and 12 show that despite this, agreement between the derived results for the "clean" Blue Streak configuration and the results for the simple Model 80 configuration is very good.

The differences between the basic Blue Streak results and the Model 80 results can thus be attributed almost entirely to the various external fitments on Blue Streak. Operationally, the most important characteristic of those under consideration is the pitching-moment slope which determines the control movement required. Fig.12 shows that so far as this characteristic is concerned each of the external fitments has an adverse effect, except the nose blister which has a negligible effect. At M=1 the stringers, pipes and nose blister account between them for about 35% of the measured difference, and the rear pods and step for the remaining 65%. The largest single item tending to increase the pitching-moment slope is the rear step. It should be noted, however, that the increment shown in Fig.12 corresponds to the case with pods already removed; if the pods are left on the effect of filling-in the step is smaller (Fig.9) as already noted.

4.4 Comparison with other tunnels at zero roll

The same Blue Streak model has been tested in the 3 ft x 3 ft Tunnel Bedford at Mach numbers of 0.7, 0.8, 0.9 and 2.0, and also in the 8 ft x 8 ft Tunnel, Bedford at Mach numbers of 1.20 to 1.73. Results of these tests are to be published separately but it is of interest to see how the present results compare with them. Figs.13 and 14 give such direct comparisons of C_Z and C_m against incidence as are possible in view of differences in configuration from the present tests, and Fig.15 compares C_Z/θ and C_m/θ at $\theta=0^\circ$ and $\theta=10^\circ$ over the Mach number range 0.7 to 2.0, with some adjustments for differences in configuration which are noted in the figures.

Comparison with the 8 ft x 8 ft Tunnel results at M=1.2, Fig.13, shows good agreement on pitching moments and fair agreement on normal-force; the present results give 4% higher normal-force slope at zero incidence and a somewhat greater non-linear lift increment. Comparison with the 3 ft x 3 ft

Tunnel results at M=0.8 and 0.9, Fig.14, also shows good agreement especially at low incidence; at high incidence there is again some tendency towards a higher non-linear lift increment in the present results. The reason for this is not known.

Results from all three tunnels are compared in Fig.15, where C_Z/θ and C_m/θ at $\theta=0^\circ$ and $\theta=10^\circ$ are plotted against Mach number. It can be seen that the various results give a consistent variation with Mach number, and the scatter is reasonably small bearing in mind the non-linearity of the basic curves and the lower experimental accuracy compared with the usual standard (para 3).

4.5 Effects of roll angle, fins off

Figs.16(a) (b) and (c) give carpets of C_Z and C_m against incidence and roll angle (up to 90°) for Mach numbers of 0.8, 1.0 and 1.2 with fins off and pipes, pods etc on. It can be seen that rolling the model increases the normal force and decreases the pitching-moment, i.e. there is an increase of lift towards the rear of the model. This is most marked near M=1.0 and least marked near M=1.2. An obvious source for this is of course the rear pods, and these would be expected to have their maximum effect at $\phi=90^\circ$. However, Fig.16 shows that the increase in normal force is greatest near $\phi=67\frac{1}{2}^\circ$, indicating that the various pipes also have some effect. Since component tests were only done at zero roll it is not possible to determine how much of the change with roll angle is due to the pods and how much to the pipes.

As noted earlier, the present tests covered only 90° of roll, and the asymmetry of the pipes and the nose blister to the model principal planes might lead to somewhat different results for roll angles beyond 90°. In this connection, some measurements have since been made up to 360° of roll in the 8 ft x 8 ft Tunnel, Bedford and some typical results are shown in Fig.21 for incidences of 6° and 10° at a Mach number of 1.19. The results are presented as polar diagrams of $-C_Z$ and C_m against roll angle, and from these diagrams it can be seen that the differences between the first quadrant and the other three are quite small. In particular, the pitching moments measured at $\phi=0^\circ$ are within 1% of the maximum recorded values (occurring at $\phi=180^\circ$, Fig.21).

4.6 Effects of fins

Figs.17(a) (b) and (c) show the effect of the fins on C_Z and C_m at Mach numbers of 0.8, 1.0 and 1.2 and roll angles of 0°, 45° and 90° (the only angles tested with fins on). The effect of the fins is non-linear with incidence and the non-linearity varies with Mach number; at M=0.8 the value of $dC_m/d\theta$ with fins on decreases quite markedly with increase of incidence, whereas at M=1.2 it tends to increase, particularly at $\phi=90^\circ$. The changes in normal-force slope and pitching-moment slope at zero incidence due to the fins are shown in Fig.18 for M=1, from which it can be seen that there is a loss of zero-incidence fin effectiveness with increase of roll angle amounting to about 23% at $\phi=90^\circ$, presumably due to interference from the rear pods. At zero roll the measured increments in normal-force and pitching-moment slopes are in quite good agreement with slender-body theory, as shown in Fig.18.

5 SIDE FORCE, YAWING MOMENT AND ROLLING MOMENT

5.1 Side force and yawing moment

As noted in para 3.1, side force and yawing moment (and also rolling moment, below) are given with respect to axes which move with the model in pitch but do not rotate with it in roll, Fig.4.

At zero roll angle the side force and yawing moment coefficients C_Y and C_n are small for all incidences and Mach numbers, the maximum numerical values being 0.05 and 0.10 respectively compared with 1.2 and 2.0 for C_Z and C_m; no results are plotted for this condition.

Rolling the model produces more or less steady variations of C_Y and C_n with incidence, with the largest increments occurring at the highest test incidence of 15°. Figs.19(a) and (b) show how these maximum or minimum values of C_Y and C_n vary with roll angle (up to 90°) at M=1. The peak values of C_Y are -0.15 with fins off and -0.22 with fins on, at a roll angle of about 25°, and the peak value of C_n is about 0.25 with fins on or off, at a roll angle of about 45°. The signs of C_Y and C_n indicate that the added side force due to roll acts near the rear of the model, but in the absence of component tests with the model rolled the relative contributions of pipes and pods are not known. The maximum measured value of C_n is about 12% of the maximum measured value of C_m.

5.2 Rolling moment

Typical $C_\ell - \theta$ curves are given in Fig.20, illustrating the effects of pipes (at zero roll), fins and roll angle.

At zero roll angle with fins off, Fig.20 shows that C_ℓ decreases with increase of incidence, reaching a value of about -0.015 at $\theta=15°$. Removal of the pipes eliminates this and gives more or less zero rolling moment throughout the incidence range.

At zero roll angle with fins on, C_ℓ is positive at all incidences and increases with incidence to a value of about 0.02 at $\theta=15°$. The change in sign and slope compared with the fins-off case must be attributed to interference from the pipes since at zero roll these are the only unsymmetrical features of the model.

The effect of rolling the model up to 90° is illustrated in Fig.20 for M=1; the behaviour at other test Mach numbers is similar. The values of C_ℓ at $\theta=15°$, M=1 are plotted against roll angle in Fig.19(c). With fins off C_ℓ reaches a maximum value of about 0.03 near $\phi=55°$; with fins on C_ℓ falls gradually from about 0.02 at $\phi=0°$ to 0.01 at $\phi=90°$.

In terms of control deflections the measured rolling moments are quite small. Thus, if it is assumed that pitch control is provided by the application of normal force 2.5 diameters behind the c.g., and roll control by circumferential force 0.5D from the axis, then at $\theta=15°$ the force required to balance the maximum measured value of C_ℓ is only about 7% of that required to balance the maximum measured value of C_m (2.0, fins off).

5.3 Higher roll angles

The above results for side force, yawing moment and rolling moment are for roll angles up to 90°. The measurements of these components in the 8 ft x 8 ft Tunnel, Bedford at higher roll angles (para 4.5) showed appreciable scatter and are not presented here. The results showed, however, that the side force, yawing moment and rolling moment remained small throughout the 360° range of roll angle.

6 AXIAL FORCE

Fig.22(a) gives the variation of the nett axial-force coefficient with Mach number at zero incidence for the three head shapes tested, and shows the effect of removing the pipes and the pods. As noted earlier, the nett axial-force coefficient is the measured value adjusted to free-stream static conditions at the base of the model by the base pressure correction ΔC_{XB}. Mean values of ΔC_{XB} are shown in Fig.22(b); the actual values vary slightly from case to case. The individual points are not shown in Fig.22(a); as discussed in para 3 there is an experimental scatter of about 0.02 in C_X about the mean curves given.

Fig.22 shows that as might be expected, the drag of the model with head A is intermediate between that with head B and that with head C. At M=1.2 the values of $(-C_X)_{nett}$ are about 0.40 for head B, 0.48 for head A and 0.56 for head C. With head C the drag is still rising at M=1.2; with the other heads it is more or less constant near M=1.2.

The pipes and pods cause significant increases in drag, particularly at the higher test Mach numbers where the pipes increase $(-C_X)_{nett}$ by about 0.035 and the pods by about 0.055. Removing the nose blister, fairing over the forward stringers, or filling in the rear step have little effect on $(-C_X)_{nett}$. In the case with step filled, however, it can be argued that the base pressure correction should be applied over the total base area (D=4") instead of, as here, over the stopped-down base area (D=3.6"); if this were done $(-C_X)_{nett}$ would be about 0.04 smaller between M=1.1 and M=1.2.

It should perhaps be noted that there is no particular operational significance in the base-pressure correction since in flight the base pressure will not in general be equal to the free-stream static pressure. Its purpose is simply to reduce experimental results, measured in the presence of an arbitrary base pressure depending on the support sting, to a known but no less arbitrary common datum. The effect on drag of filling-in the rear step on the full-scale missile may be quite different from that measured here, with or without the base pressure correction; this is particularly so with rocket efflux present.

7 CONCLUSIONS

The results show that with fins off the static stability characteristics of the tested Blue Streak model are free from serious irregularities at Mach numbers of 0.80 to 1.25, roll angles up to 90° and incidences up to 15°, and the pitching moment is roughly linear with incidence about the full-scale centre-of-gravity position for this Mach number range. With fins on there is some non-linearity, particularly at subsonic speeds.

At zero incidence the values of $dC_m/d\theta$ are greater than was expected from earlier tests on simple cone-cylinders. The discrepancy is greatest near M=1 where it amounts to about 28% for the chosen axis position.

Component tests show that the increase is entirely attributable to the various external fitments, all of which increase $dC_m/d\theta$.

The induced rolling moment, and the yawing moment and side force (in a plane normal to the body incidence plane) are fairly small for all test conditions.

Good agreement is obtained, after adjustment for model differences, between the present results, the results obtained on the same model in the 3 ft x 3 ft and 8 ft x 8 ft Tunnels, Bedford, and the earlier Model 80 cone-cylinder tests.

Printed in England for Her Majesty's Stationery Office by the Royal Aircraft Establishment, Farnborough. W.T.60.K.4.

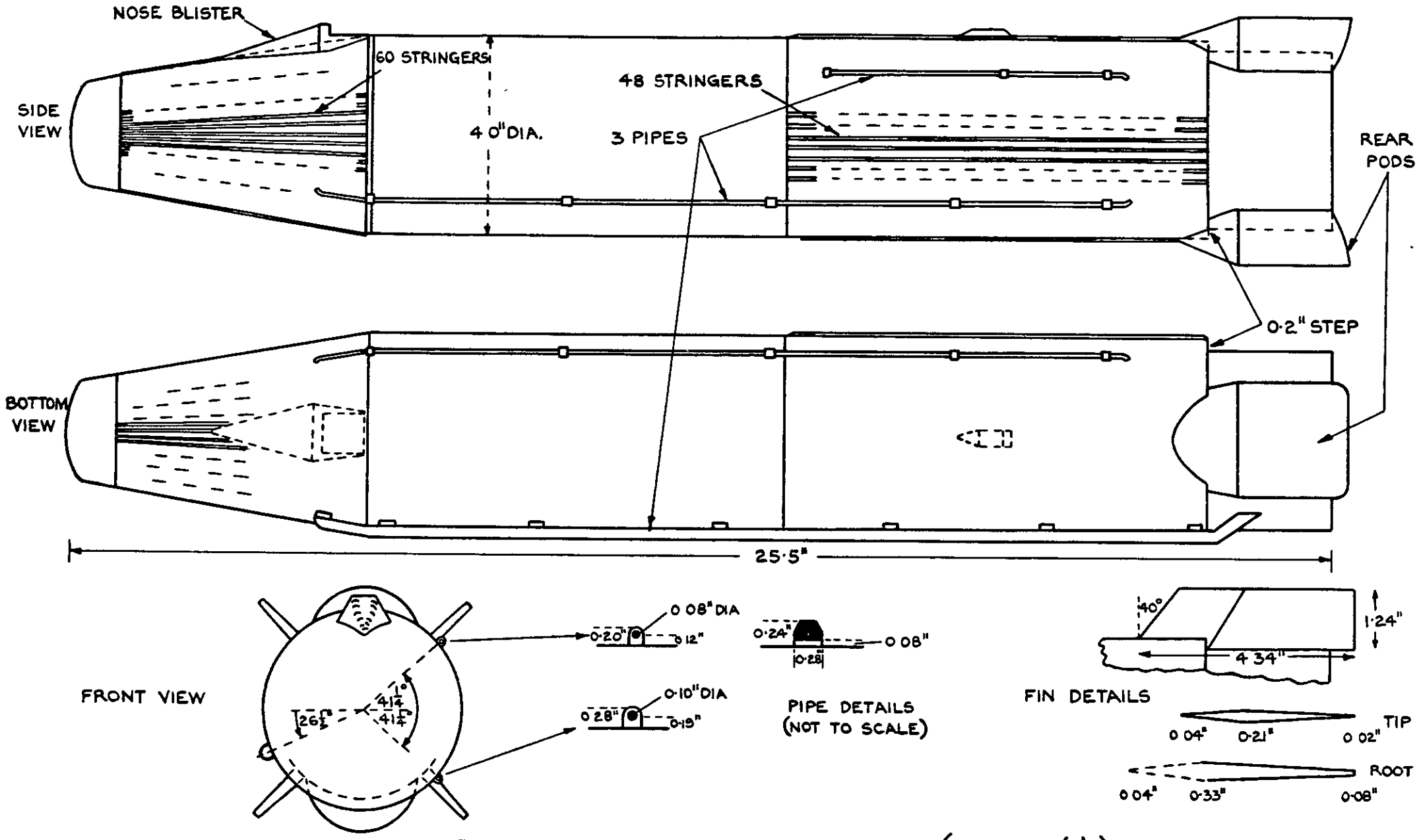

FIG. 1. DETAILS OF MODEL (HEAD 'A')

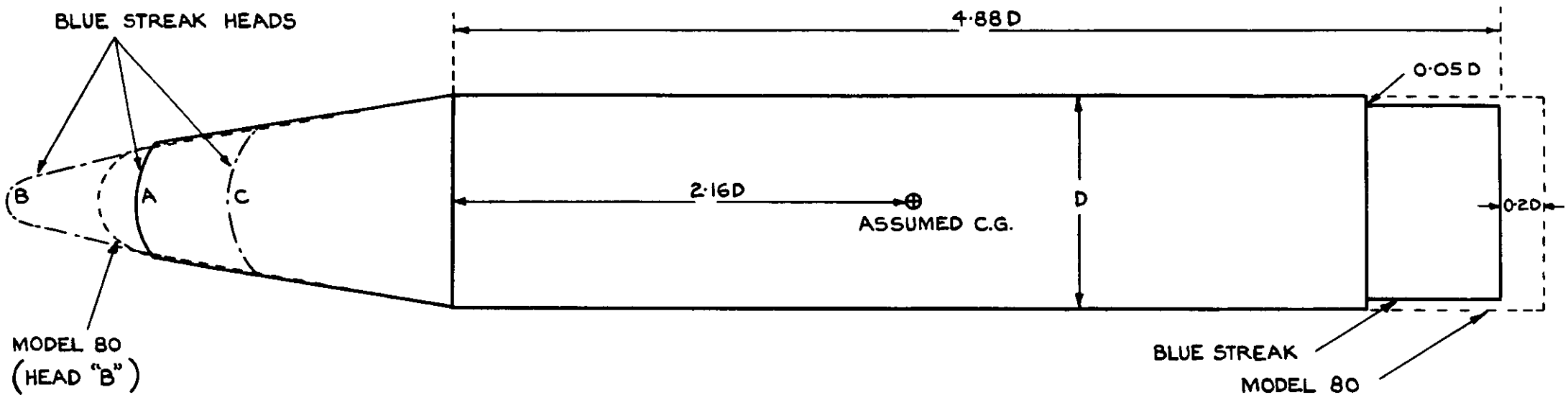

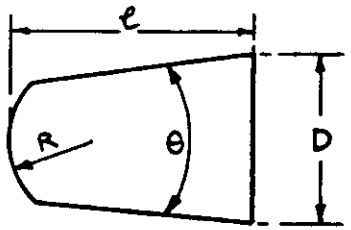

		R/D	ℓ/D	θ°	BLOCKAGE
BLUE STREAK	HEAD A	0·544	1·50	19·4	0·18%
	HEAD B	0·100	2·10	30·2 – 19·4	"
	HEAD C	0·495	1·07	19·4	"
MODEL 80	HEAD "B"	0·250	1·65	20	0·38%

FIG.2. MODEL HEAD SHAPES AND DIMENSIONS; COMPARISON WITH MODEL 80.

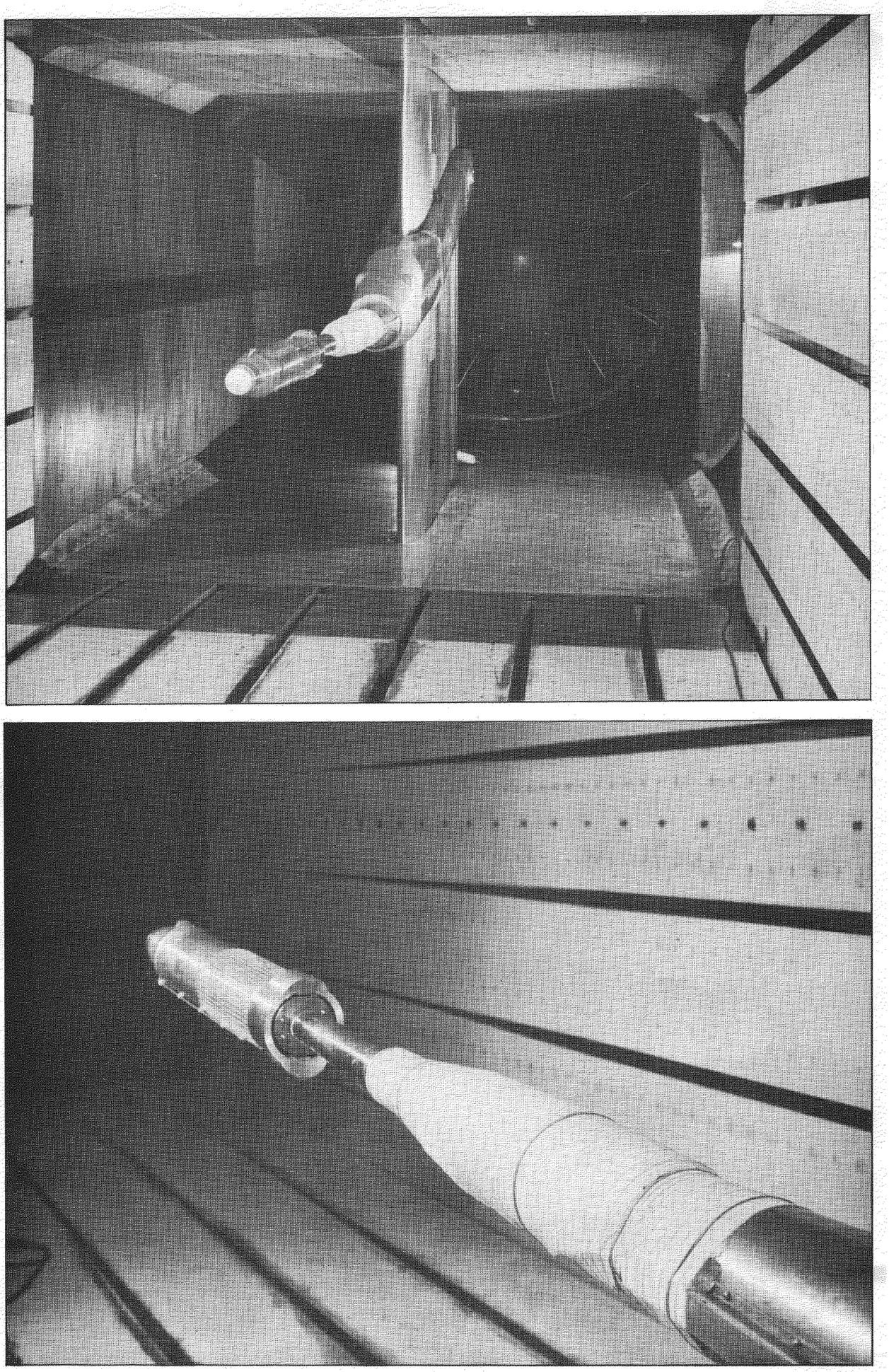

FIG.3. MODEL MOUNTED IN 8 ft. x 6 ft. TUNNEL

AXES MOVE WITH MODEL IN PITCH
BUT NOT IN ROLL.

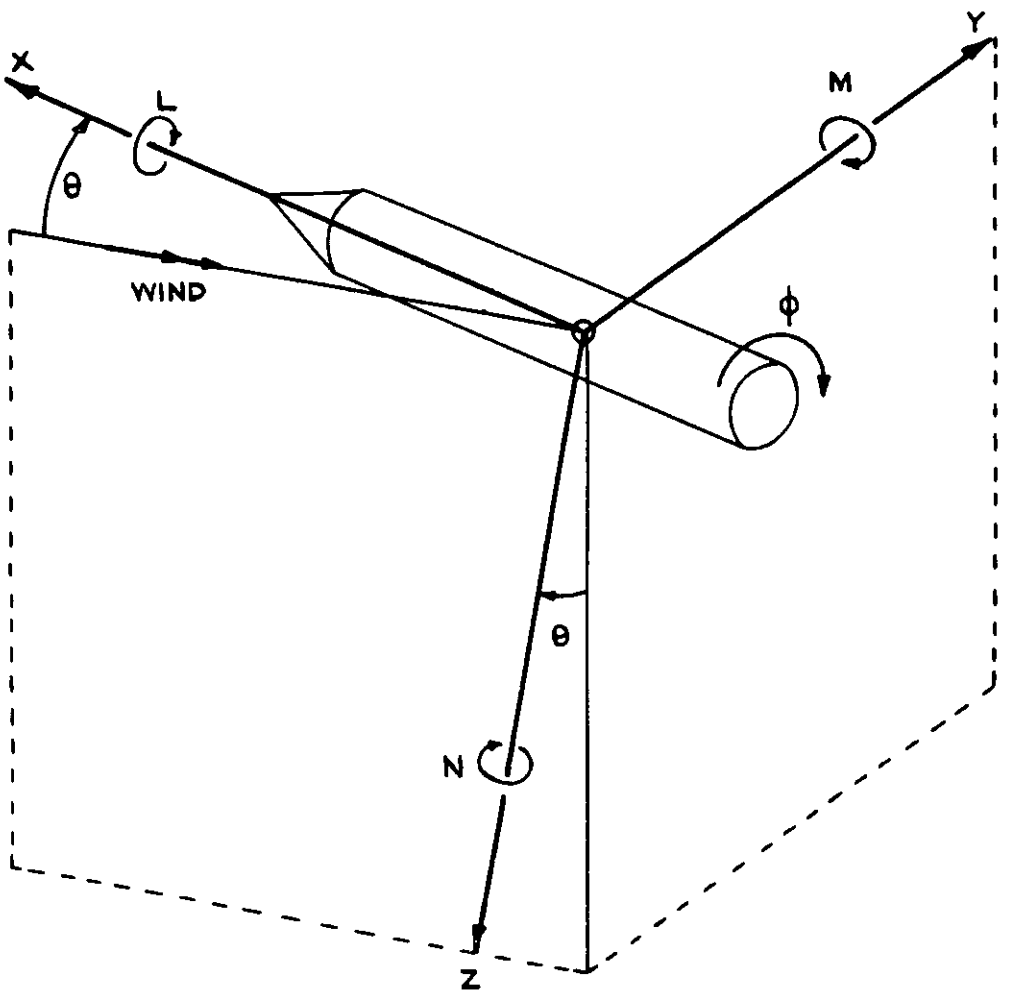

FIG.4. AXIS SYSTEM, SHOWING POSITIVE DIRECTIONS OF FORCES AND MOMENTS (PARA.3).

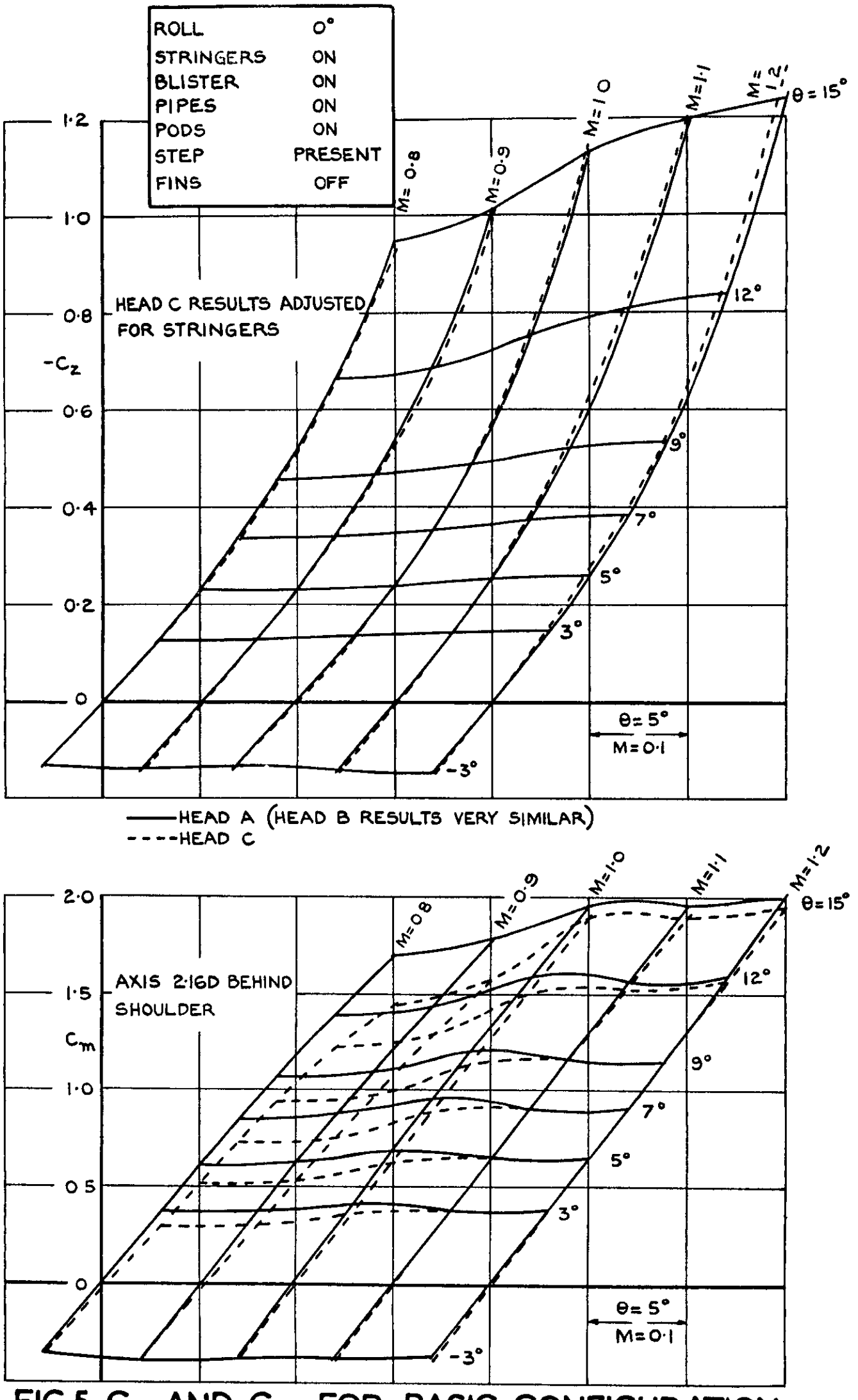

FIG.5. C_z AND C_m FOR BASIC CONFIGURATION, AND EFFECT OF HEAD SHAPE (PARAS. 4.1, 4.2).

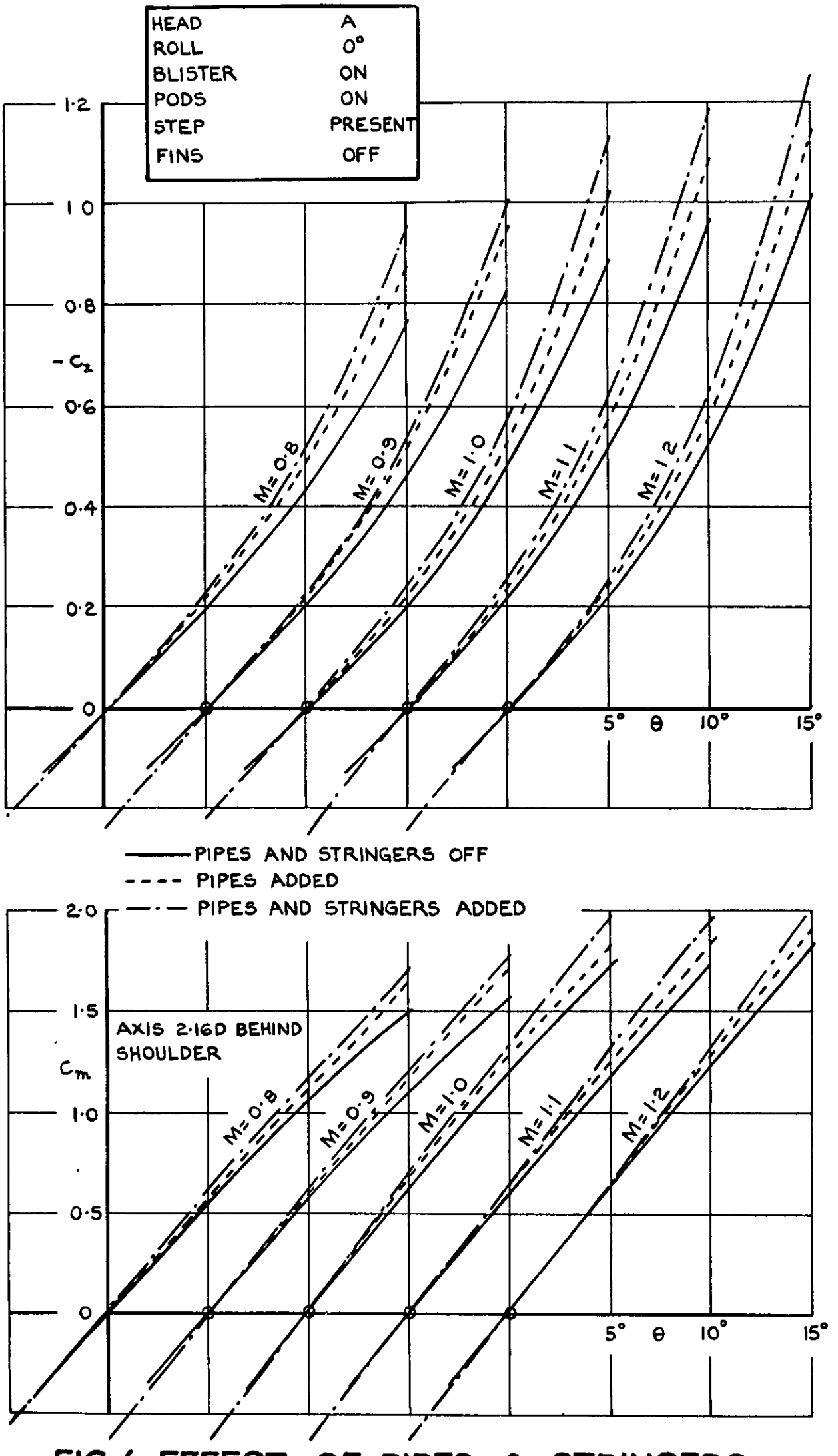

FIG. 6. EFFECT OF PIPES & STRINGERS ON C_z & C_m (PARA. 4.2)

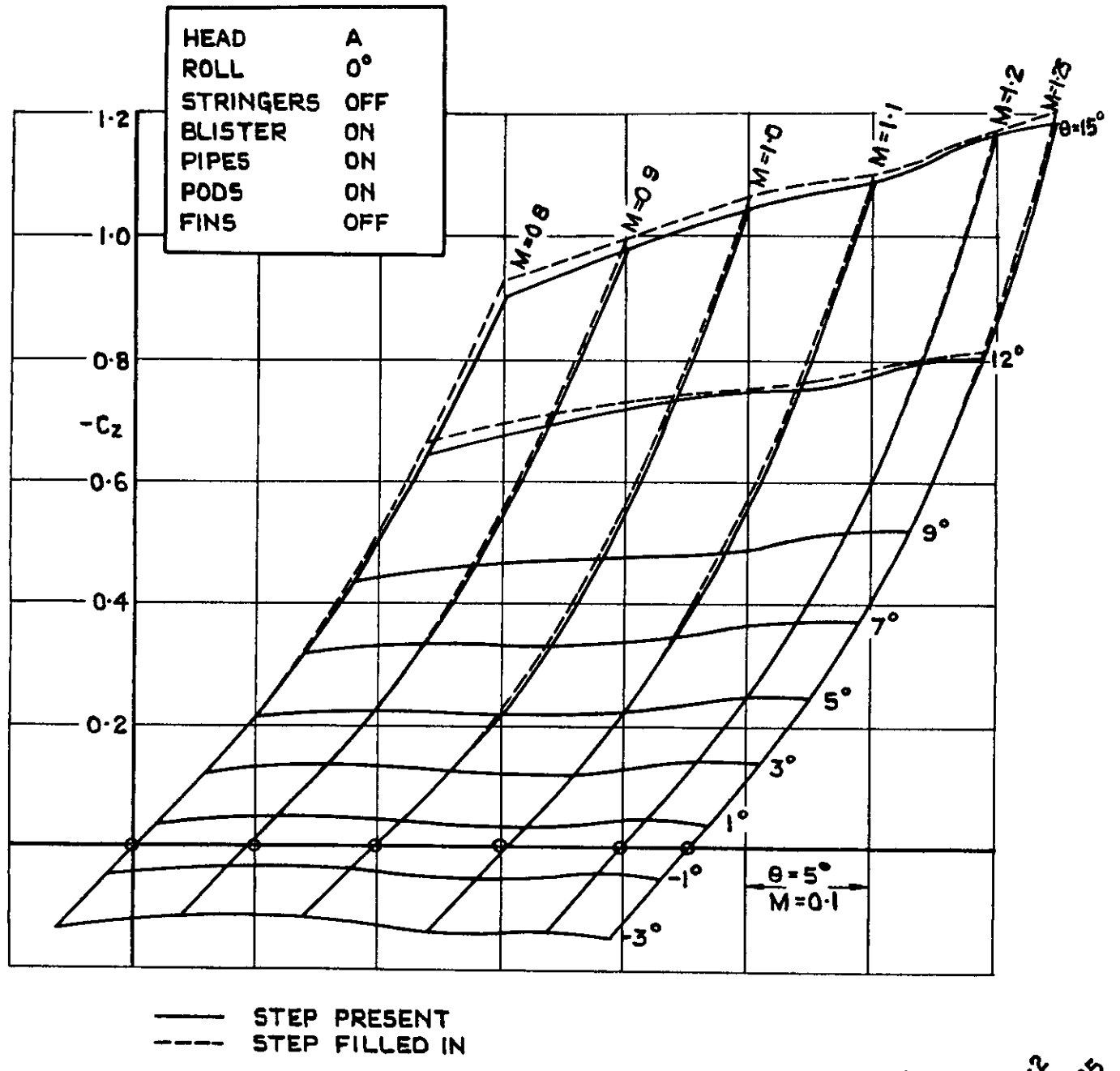

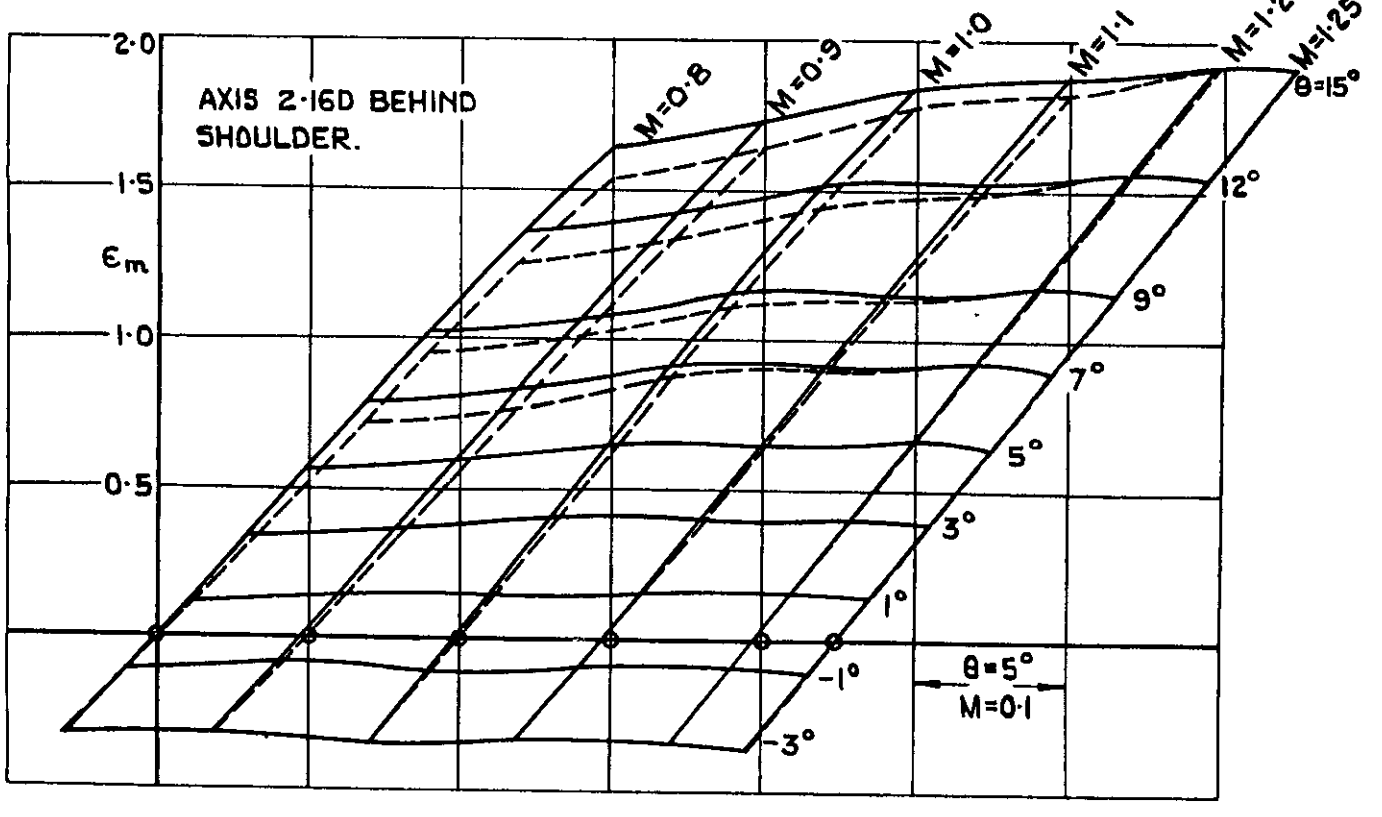

(a) PODS ON

FIG. 7(a) EFFECT OF REAR STEP ON C_z & C_m (PARA. 4.2)

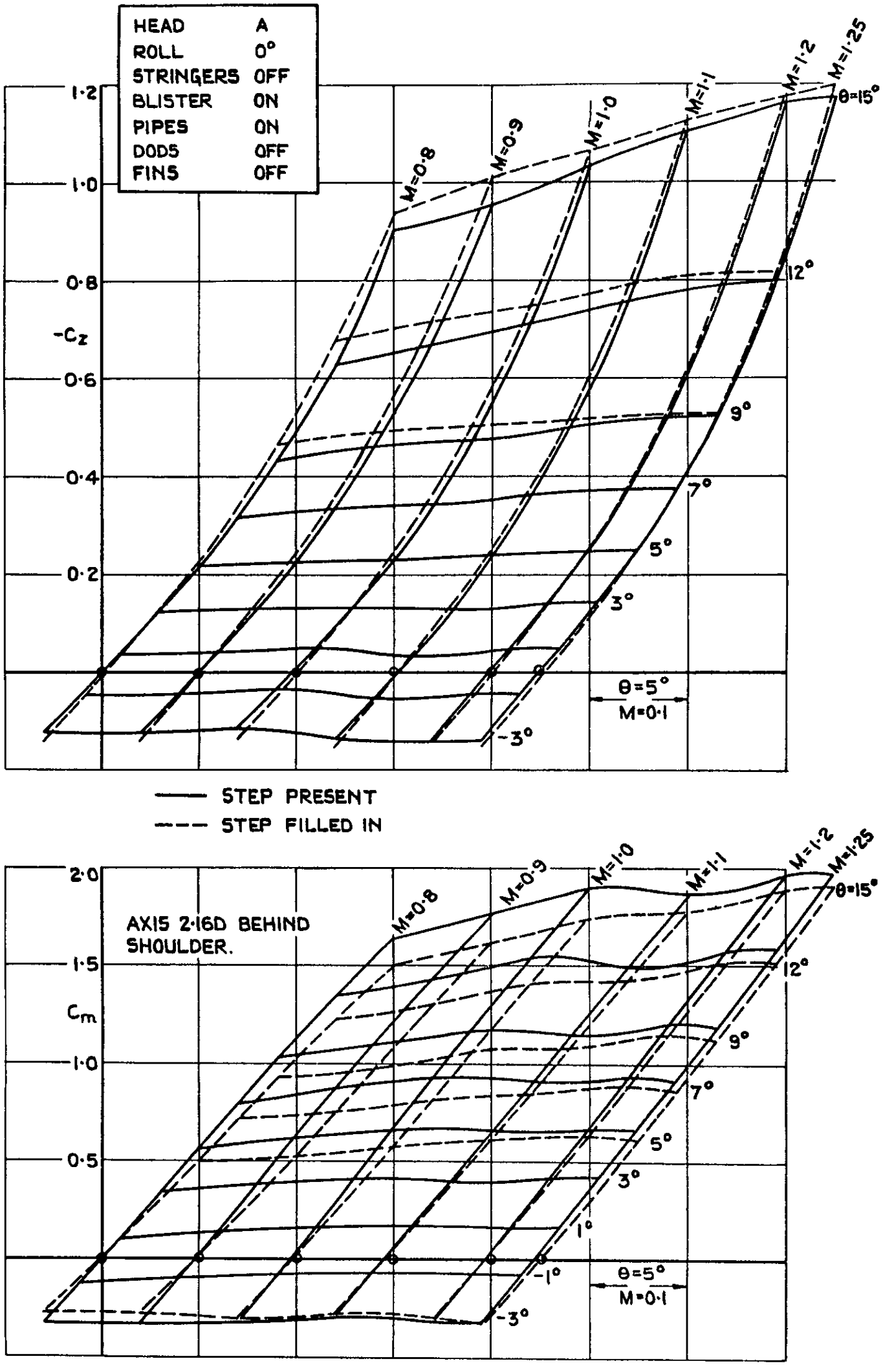

(b) PODS OFF

FIG. 7 (b) EFFECT OF REAR STEP ON C_z & C_m.

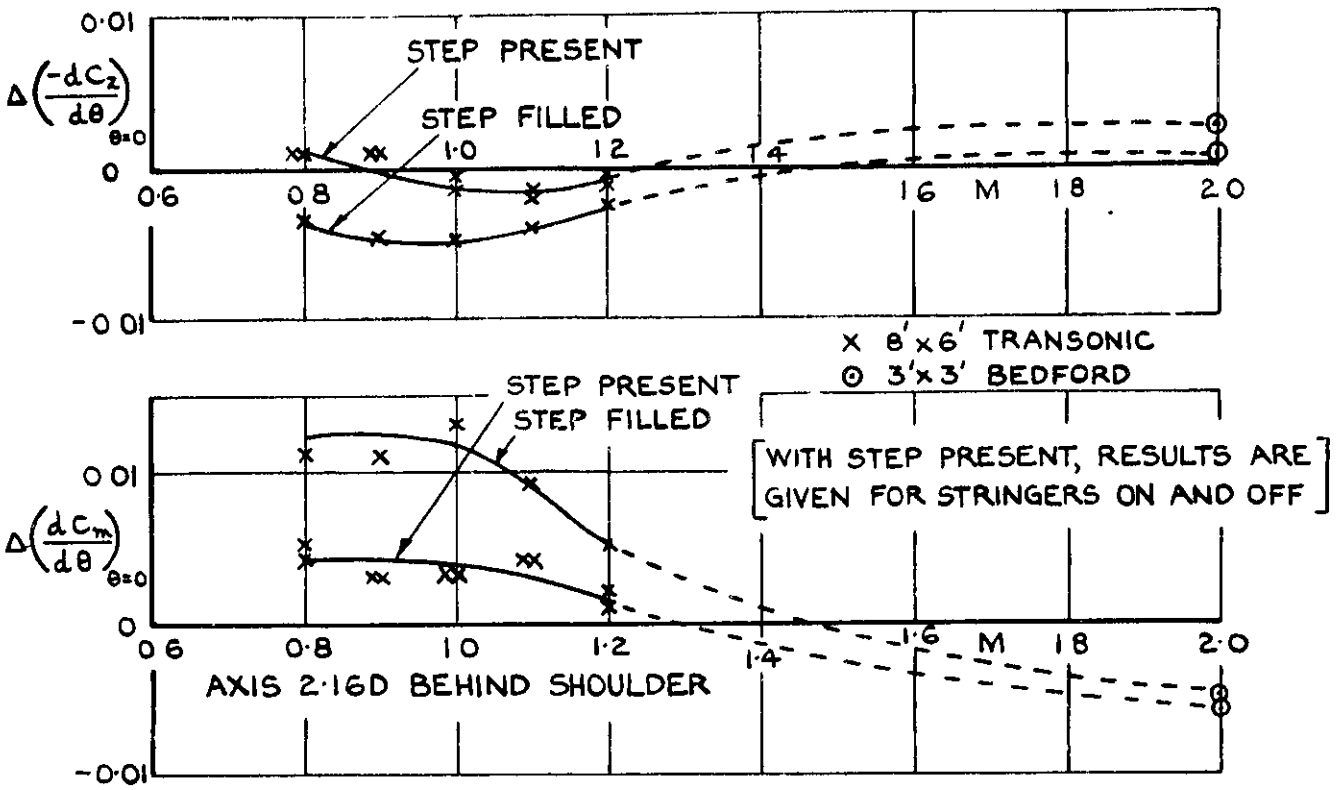

FIG.8. INCREMENTS IN $(-dC_z/d\theta)$ AND $(dC_m/d\theta)$ DUE TO REAR PODS (PARAS. 4.2, 4.3)

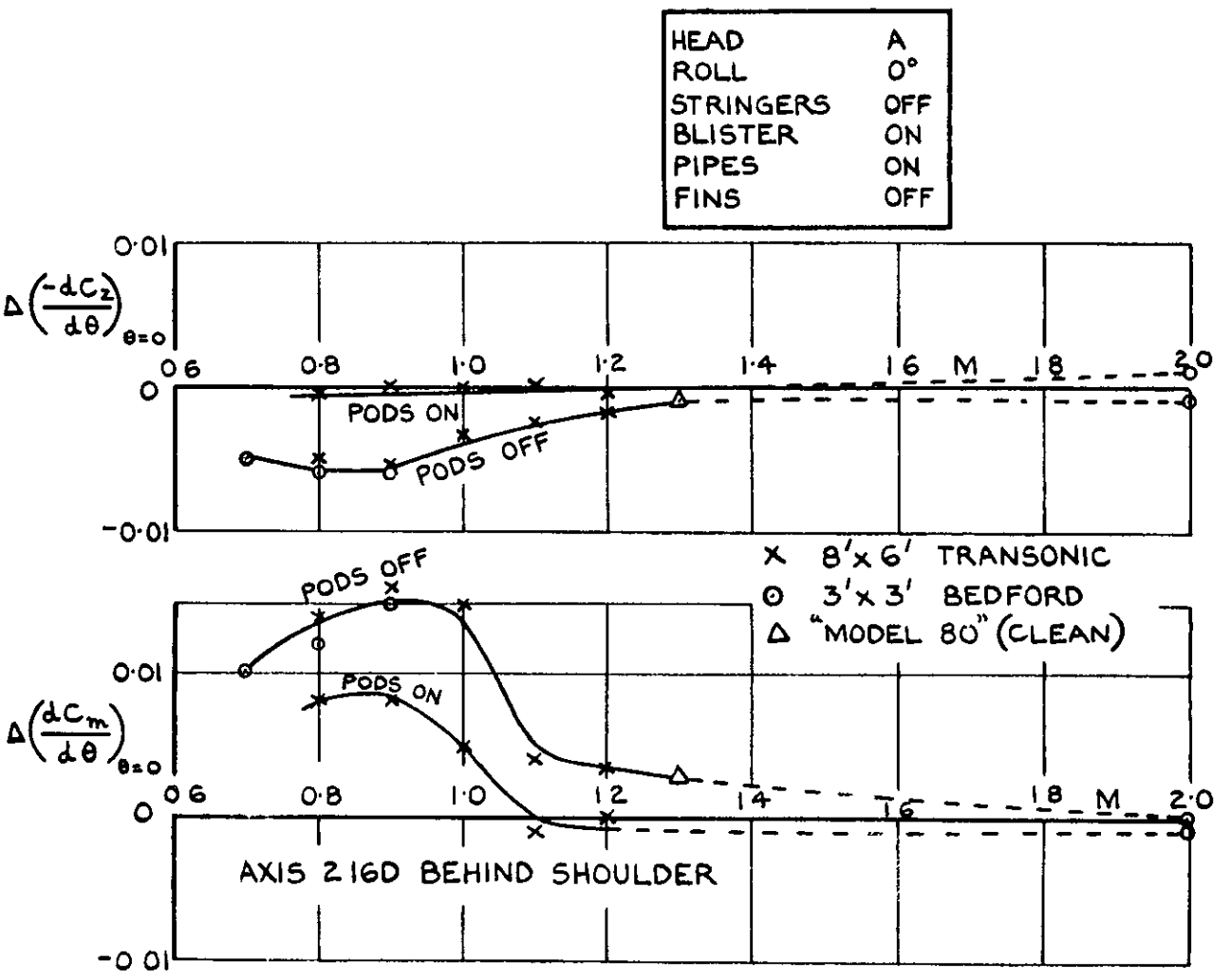

FIG.9. INCREMENTS IN $(-dC_z/d\theta)$ AND $(dC_m/d\theta)$ DUE TO PRESENCE OF REAR STEP (PARAS. 4.2, 4.3)

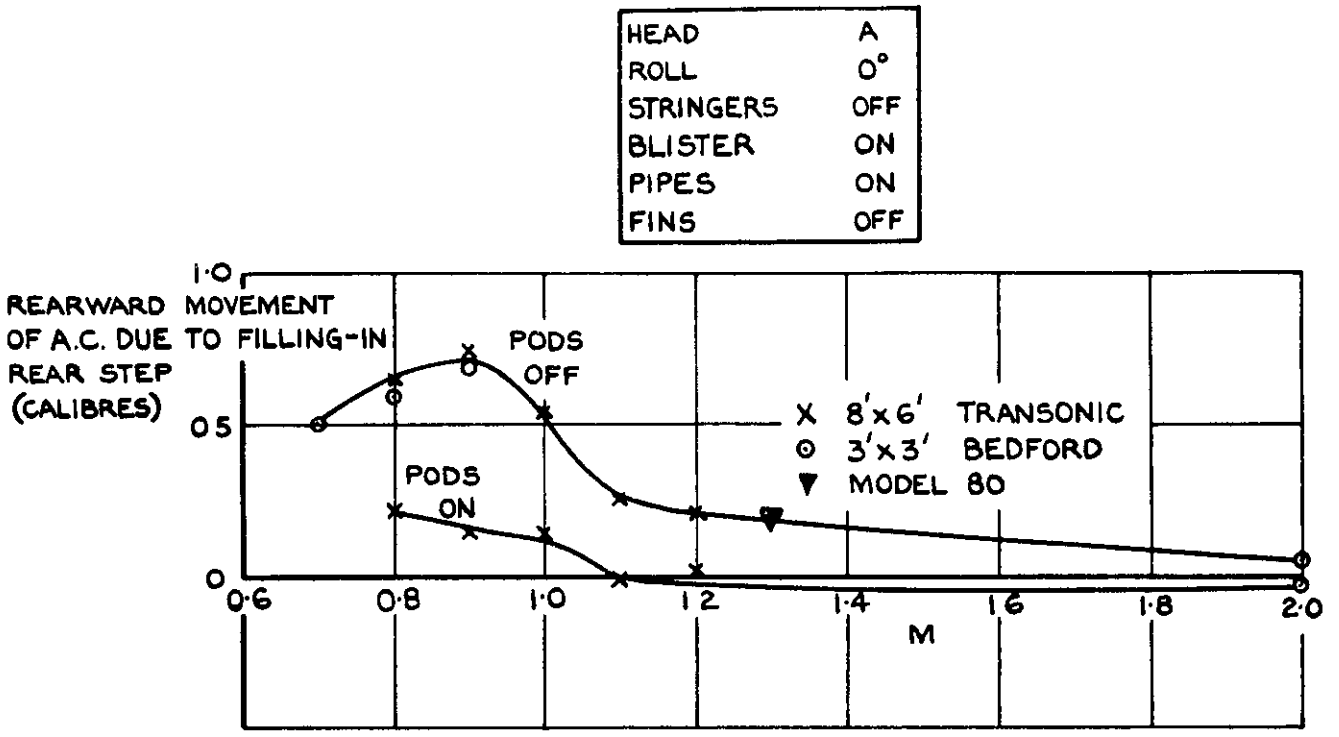

FIG. 10. AERODYNAMIC CENTRE MOVEMENT DUE TO FILLING - IN REAR STEP (PARA. 4.2).

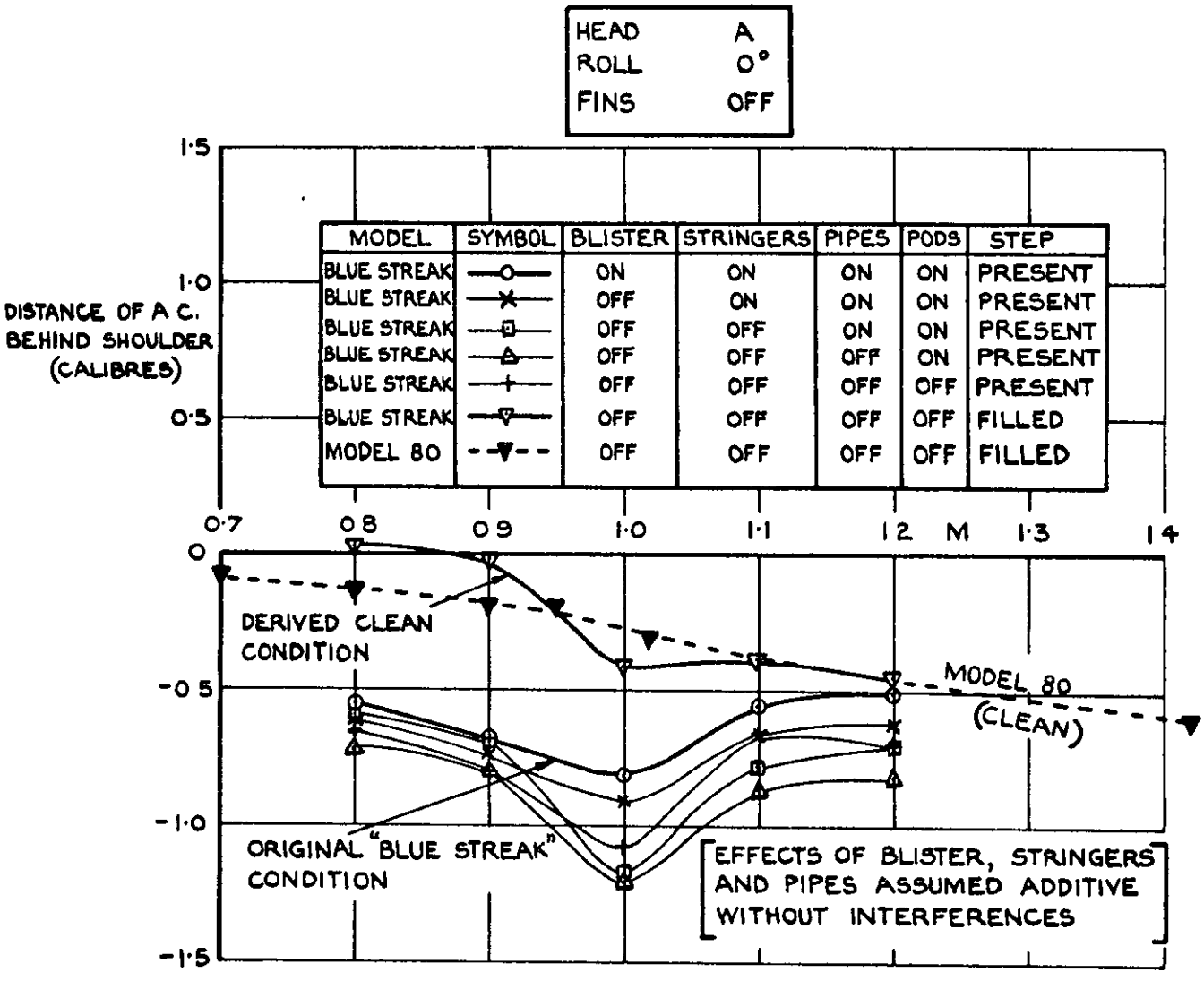

FIG.11. AERODYNAMIC CENTRE POSITION. APPROXIMATE EFFECTS OF REMOVING COMPONENTS AND COMPARISON WITH "MODEL 80" CLEAN CONDITION (PARA. 4).

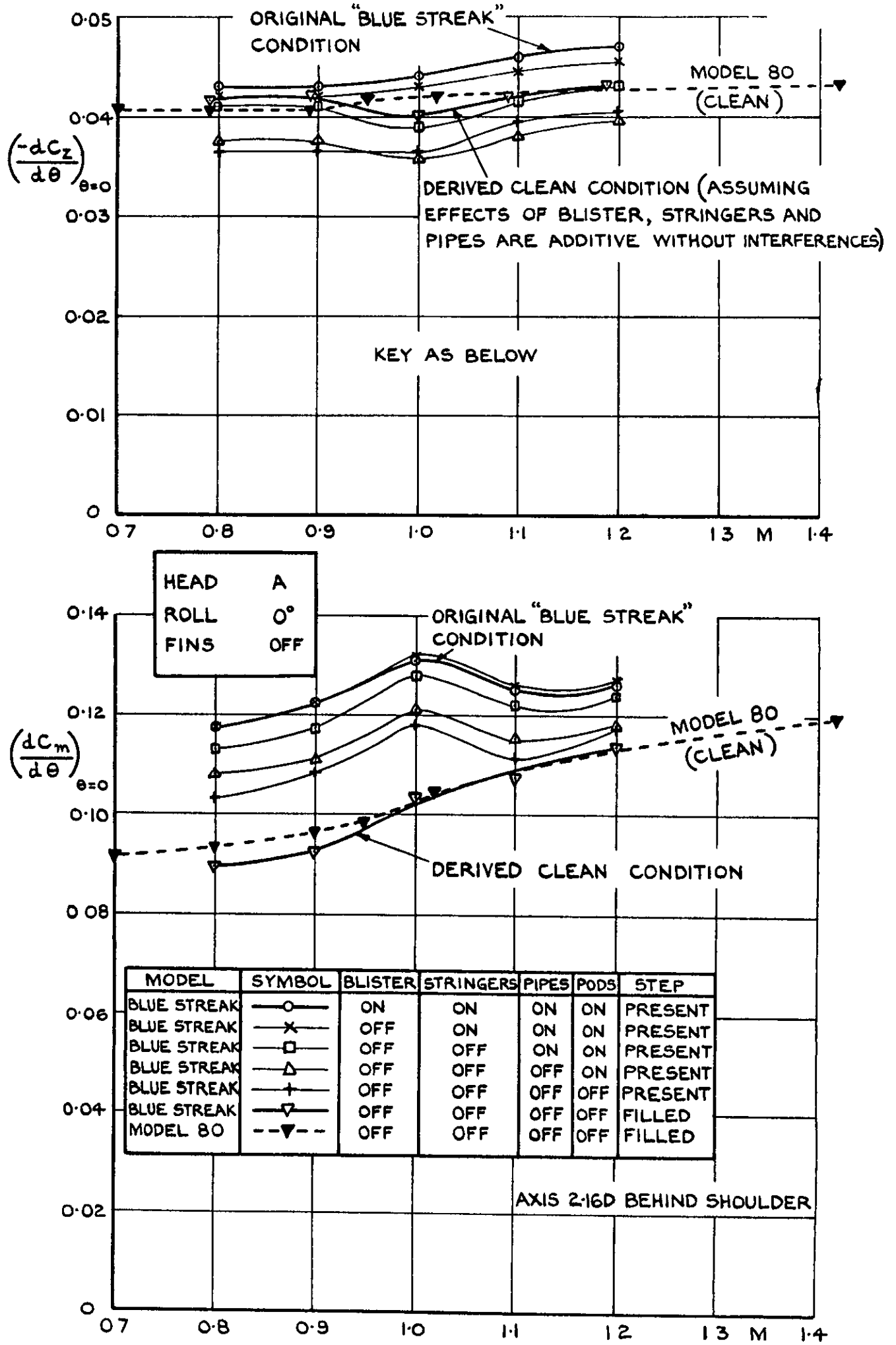

MODEL	SYMBOL	BLISTER	STRINGERS	PIPES	PODS	STEP
BLUE STREAK	—○—	ON	ON	ON	ON	PRESENT
BLUE STREAK	—×—	OFF	ON	ON	ON	PRESENT
BLUE STREAK	—□—	OFF	OFF	ON	ON	PRESENT
BLUE STREAK	—△—	OFF	OFF	OFF	ON	PRESENT
BLUE STREAK	—+—	OFF	OFF	OFF	OFF	PRESENT
BLUE STREAK	—▽—	OFF	OFF	OFF	OFF	FILLED
MODEL 80	--▼--	OFF	OFF	OFF	OFF	FILLED

FIG.12. $dC_z/d\theta$ AND $dC_m/d\theta$ AT $\theta = 0$. EFFECT OF REMOVING COMPONENTS IN TURN, AND COMPARISON WITH "MODEL 80" CLEAN CONFIGURATION (PARA.4).

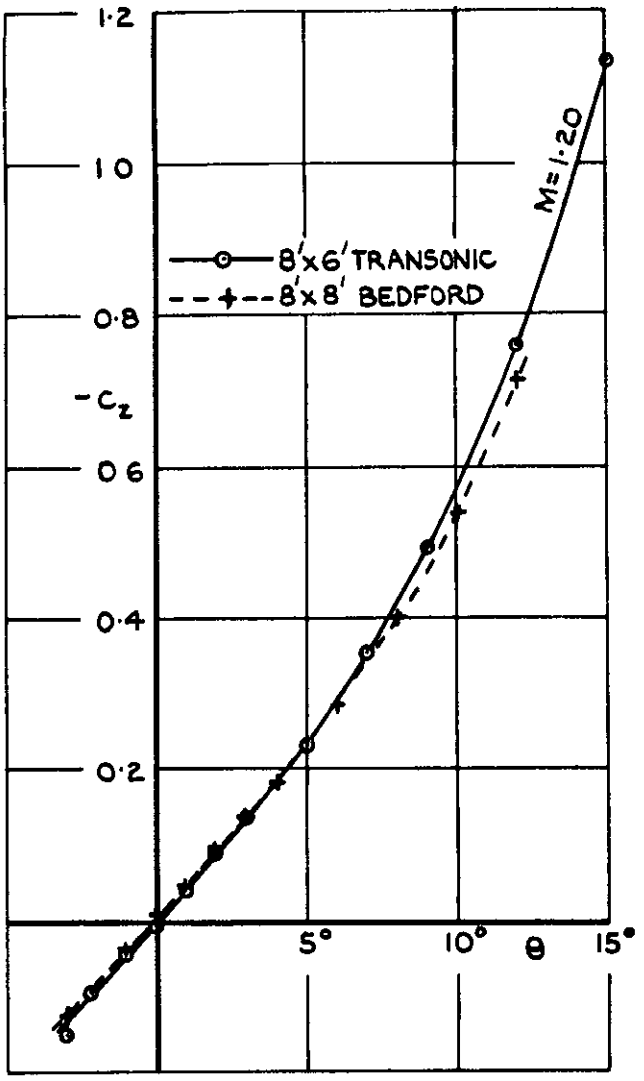

HEAD	A
ROLL	0°
STRINGERS	OFF
BLISTER	OFF
PIPES	ON
PODS	ON
STEP	FILLED
FINS	OFF

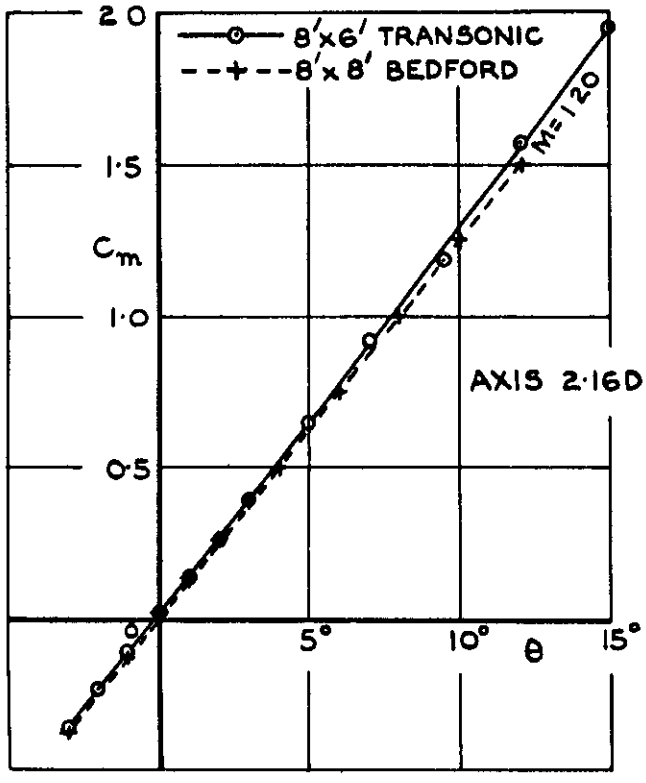

⊙ 8′×6′ RESULTS ADJUSTED FOR BLISTER

AXIS 2·16D BEHIND SHOULDER

FIG. 13. C_z vs θ AND C_m vs θ. COMPARISON WITH 8′ × 8′ (BEDFORD) RESULTS AT M=1·20 (PARA. 4.4).

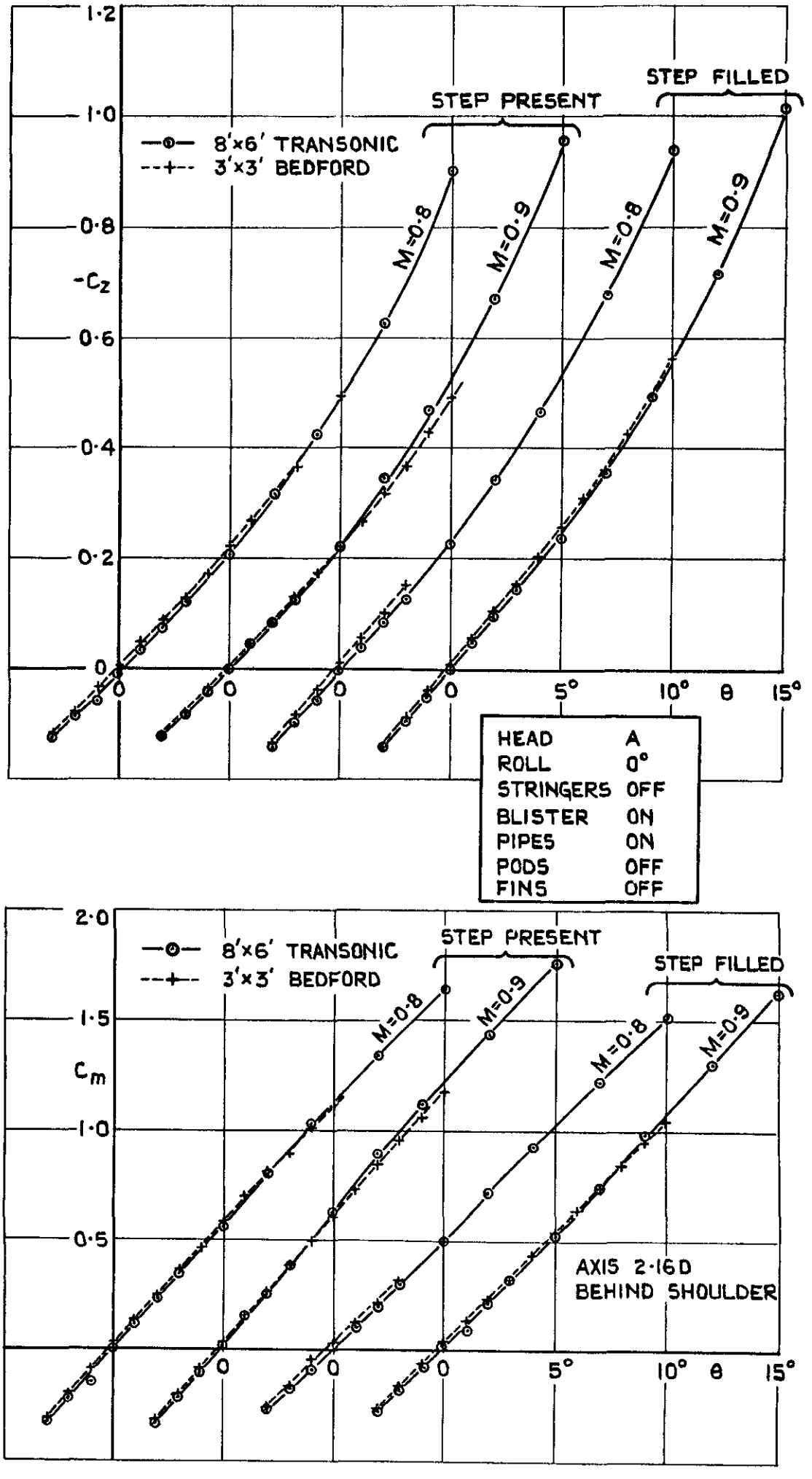

FIG. 14 C_z vs θ AND C_m vs θ. COMPARISON WITH 3'x3' (BEDFORD) RESULTS AT M=0·8, 0·9. (PARA 4.4)

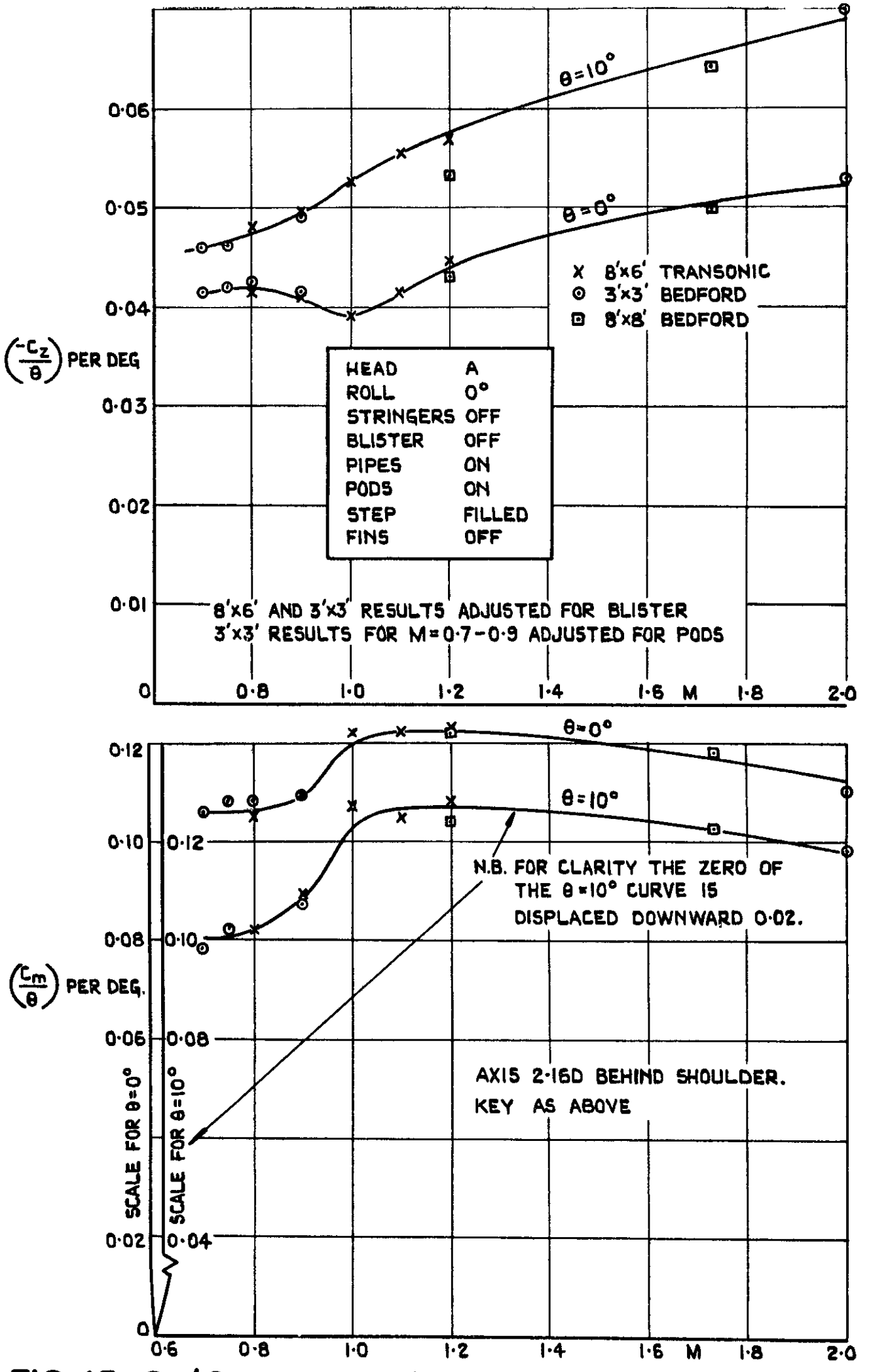

FIG. 15 C_z/θ AND C_m/θ vs. M. COMPARISON OF RESULTS FROM 8'x6', 8'x8' AND 3'x3' TUNNELS. (PARA. 4.4)

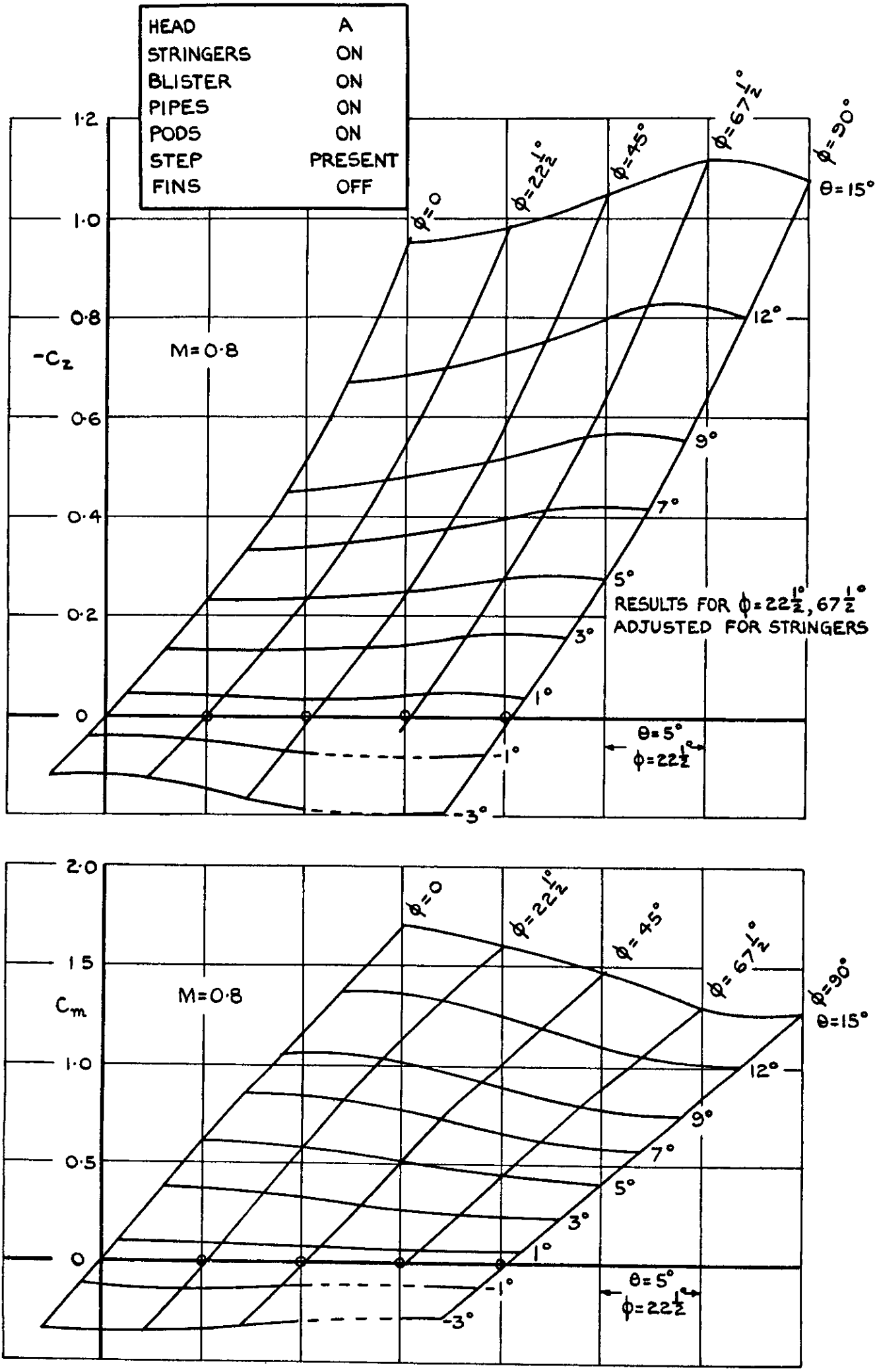

(a) M = 0·8

FIG.16 (a). C_z & C_m FOR VARIOUS ROLL ANGLES, FINS OFF (PARA. 4.5).

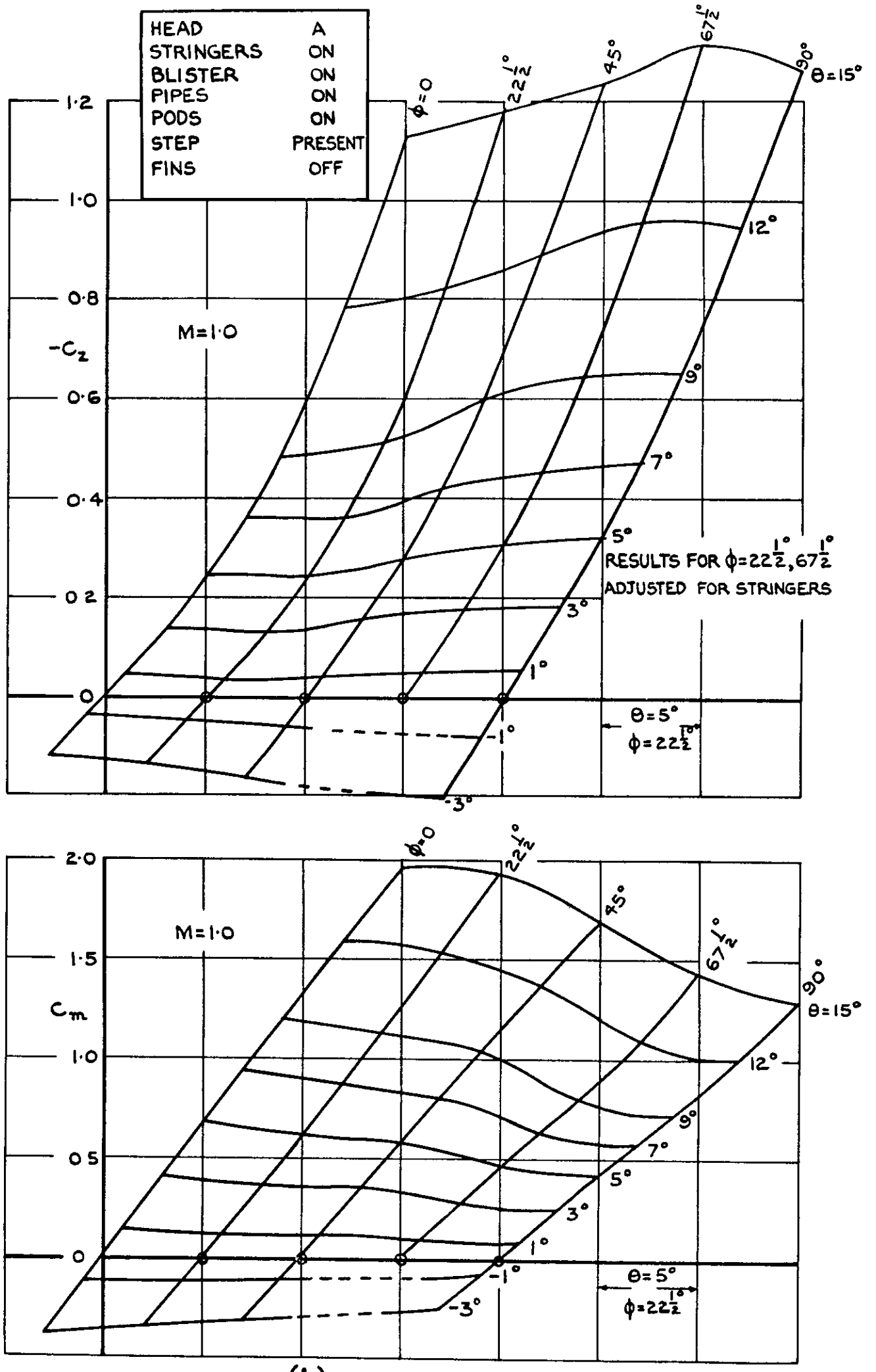

(b) M = 1·0

FIG.16(b). C_z & C_m FOR VARIOUS ROLL ANGLES, FINS OFF.

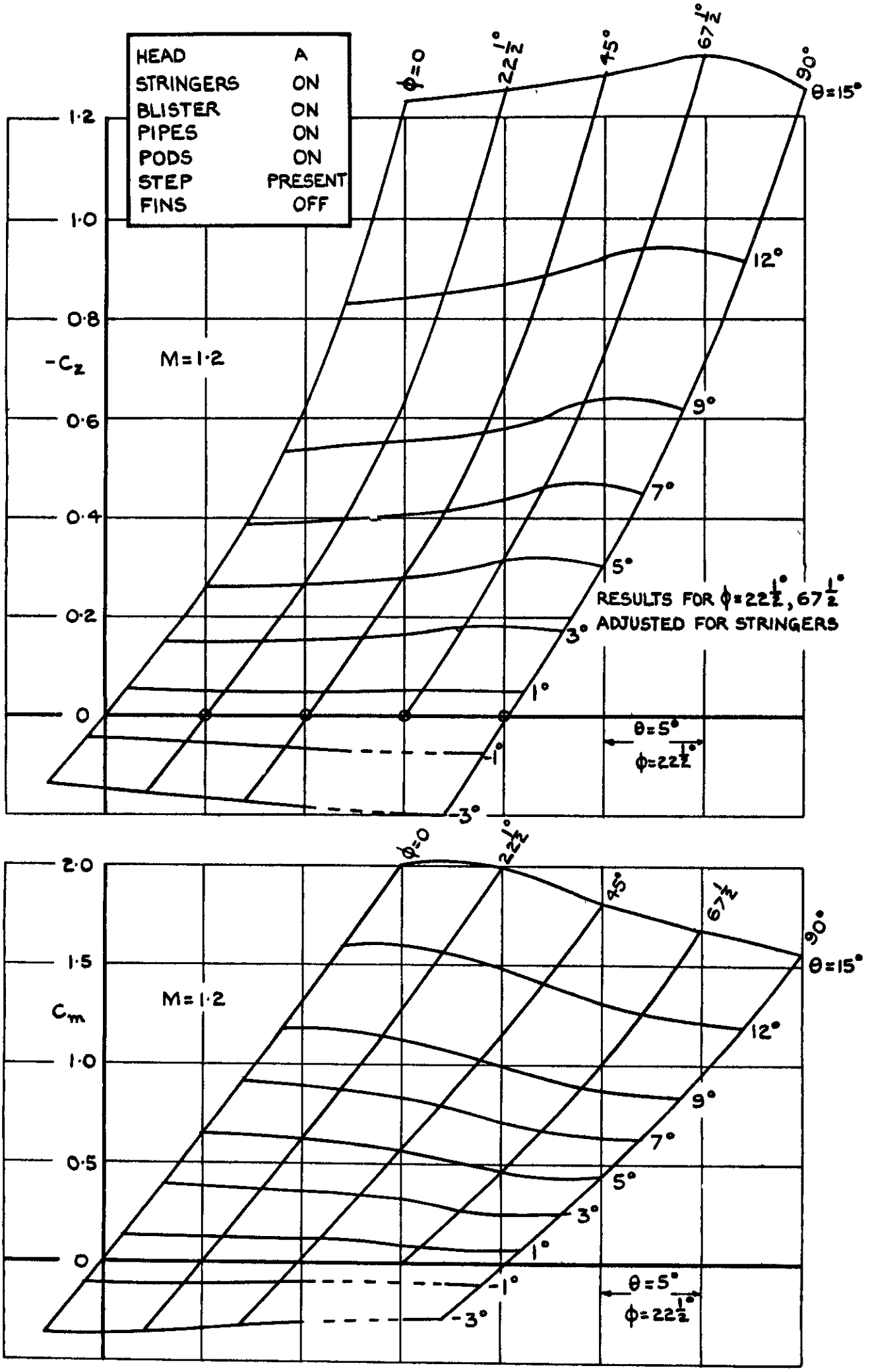

(c) M=1·2

FIG. 16 (c). C_z & C_m FOR VARIOUS ROLL ANGLES, FINS OFF.

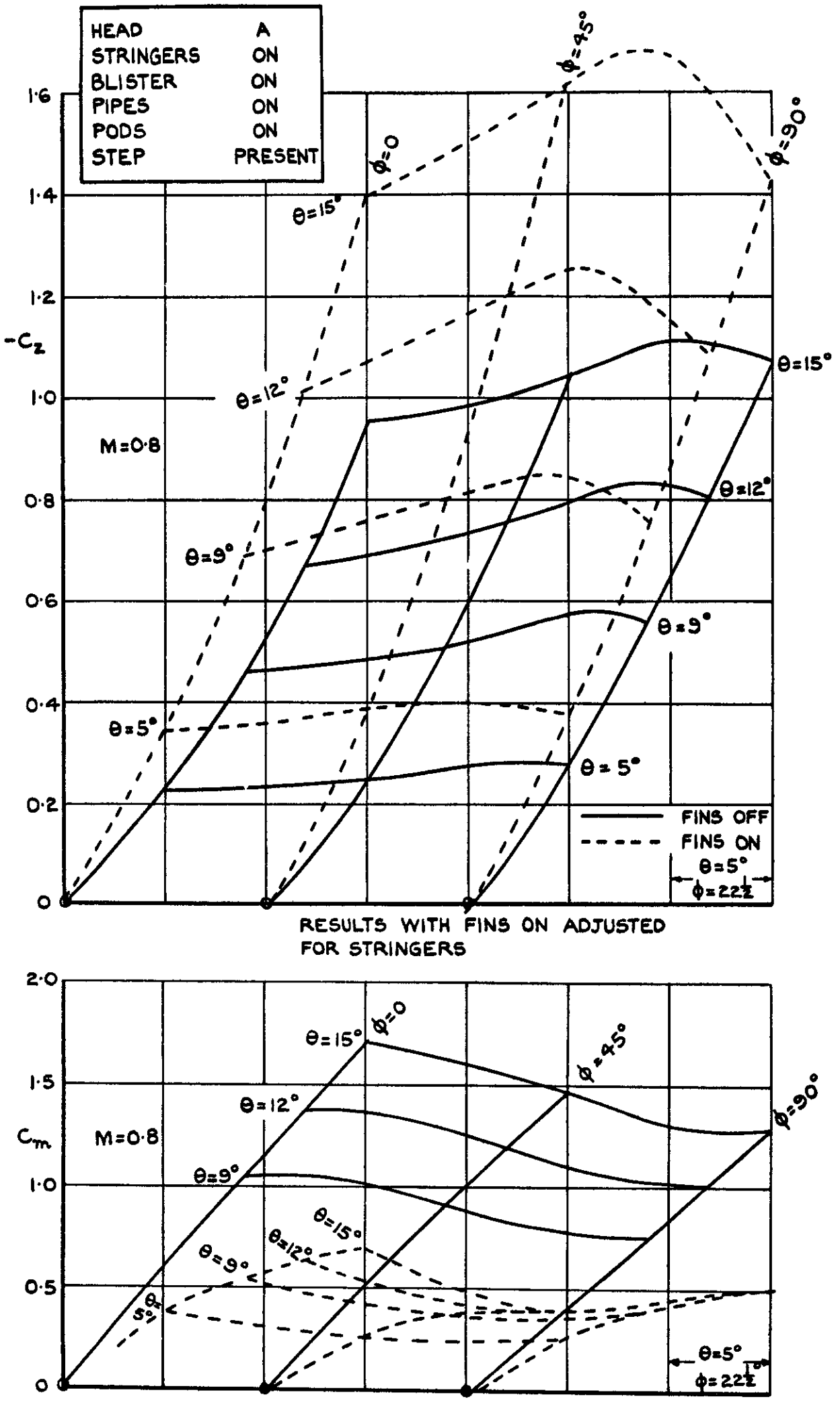

(a) M=0·8

FIG.17(a). EFFECT OF FINS ON C_z & C_m FOR VARIOUS ROLL ANGLES (PARA. 4.6).

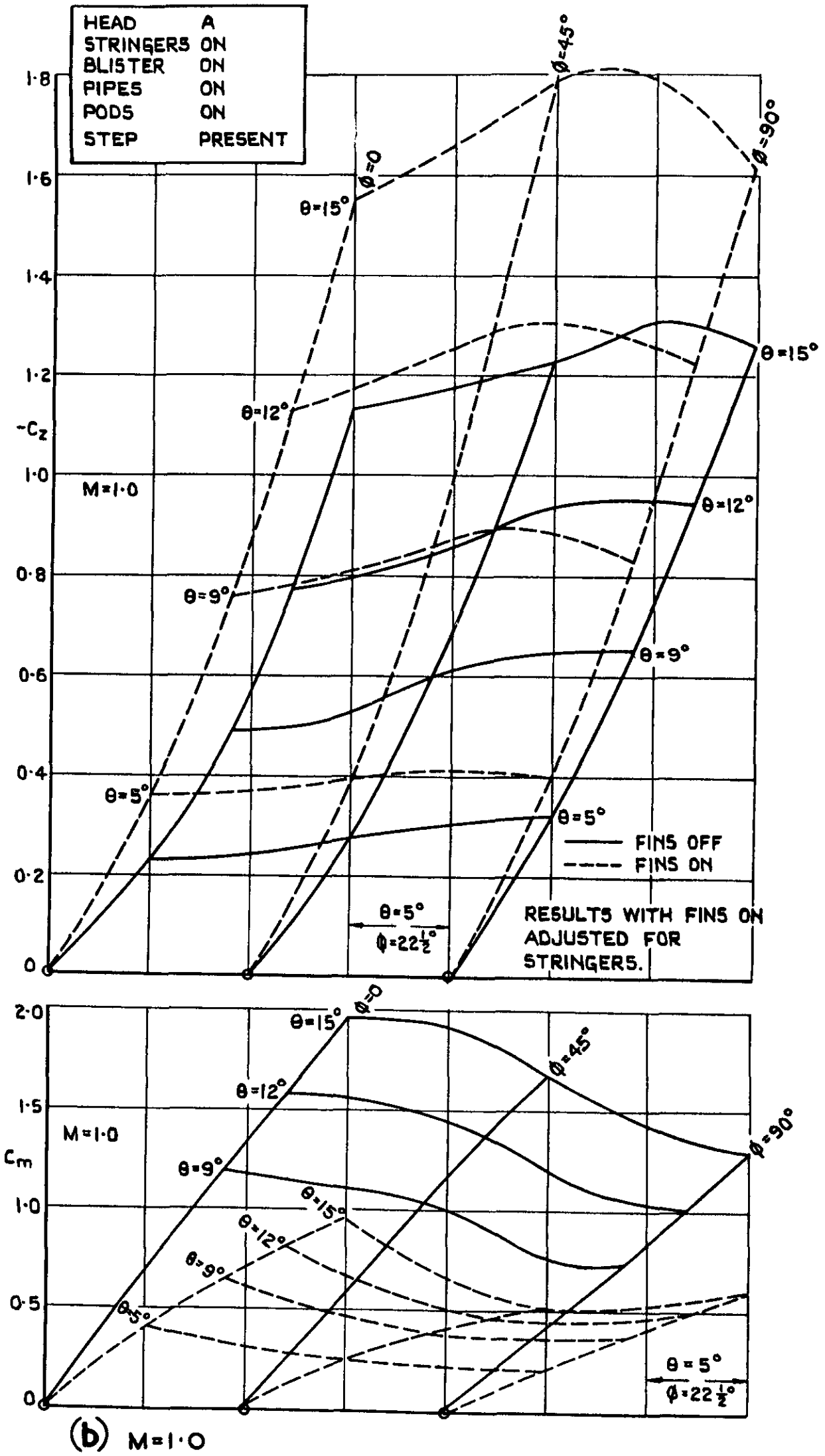

(b) M=1·0

FIG. 17(b) EFFECT OF FINS ON C_z & C_m FOR VARIOUS ROLL ANGLES.

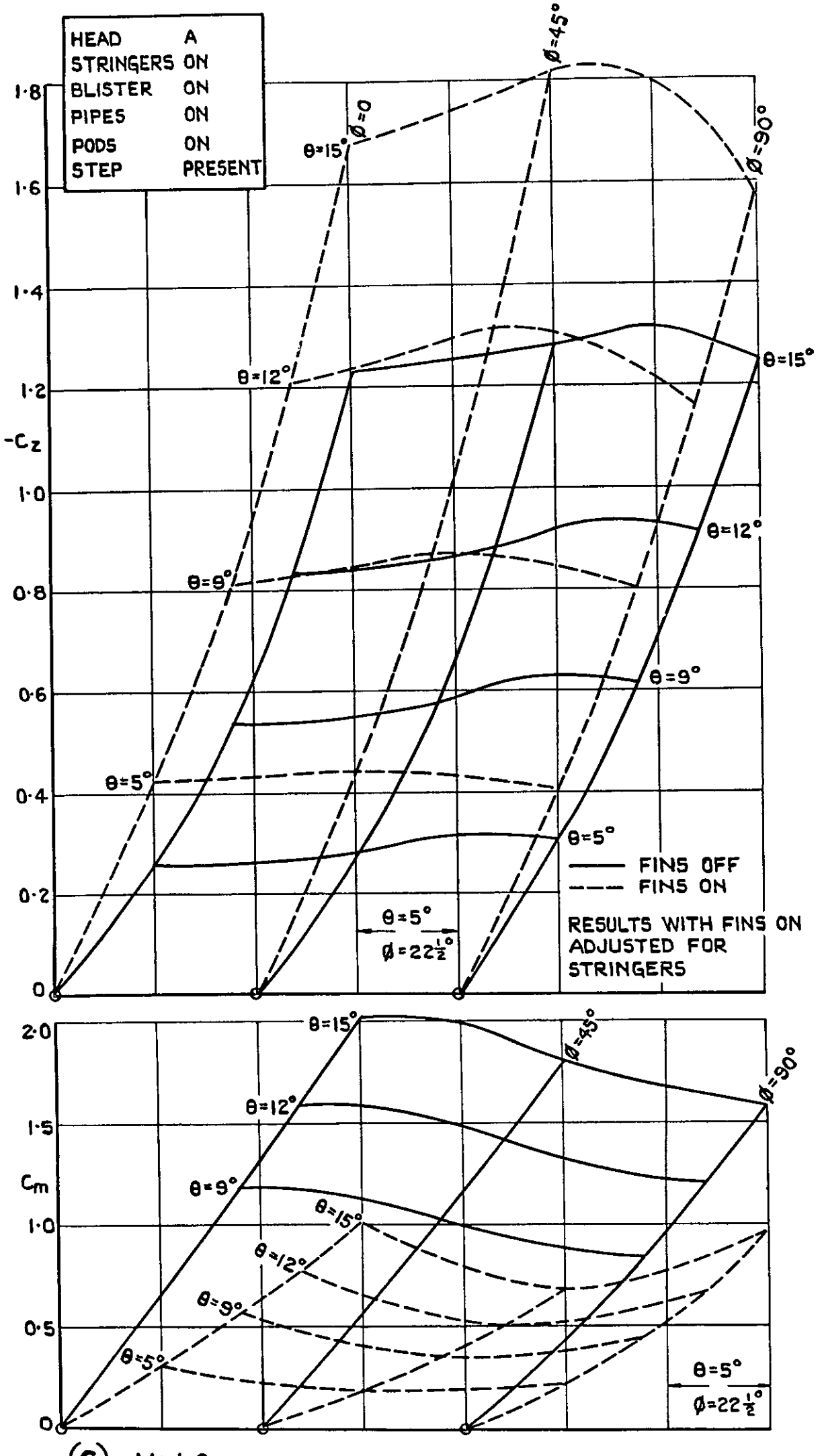

(c) M=1·2.

FIG. 17 (c) EFFECT OF FINS ON C_z & C_m FOR VARIOUS ROLL ANGLES.

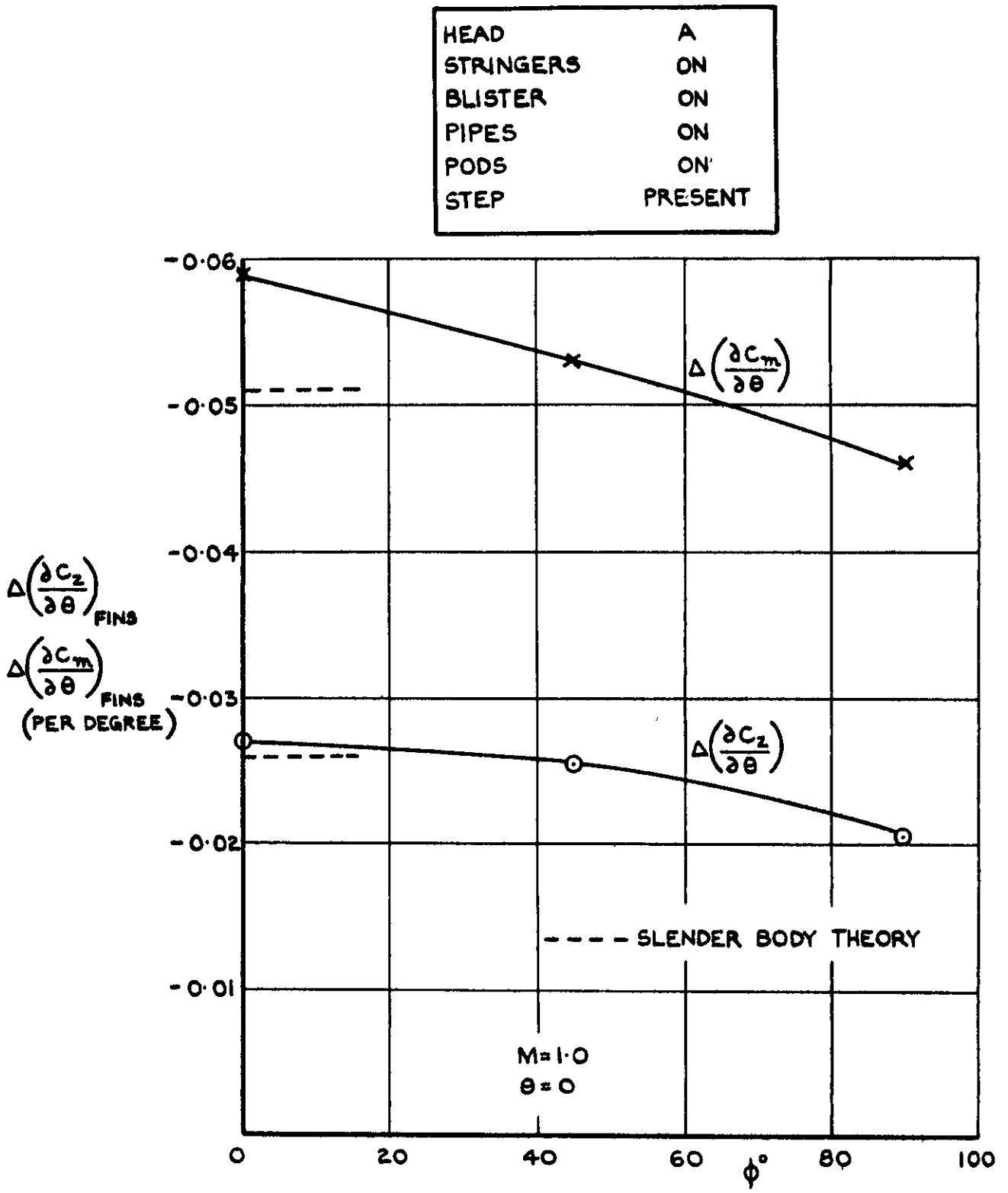

FIG. 18. INCREASES IN NORMAL-FORCE SLOPE AND STABILITY DUE TO FINS AT M=1·0, θ=0 AND VARIOUS ROLL ANGLES. (PARA. 4.6).

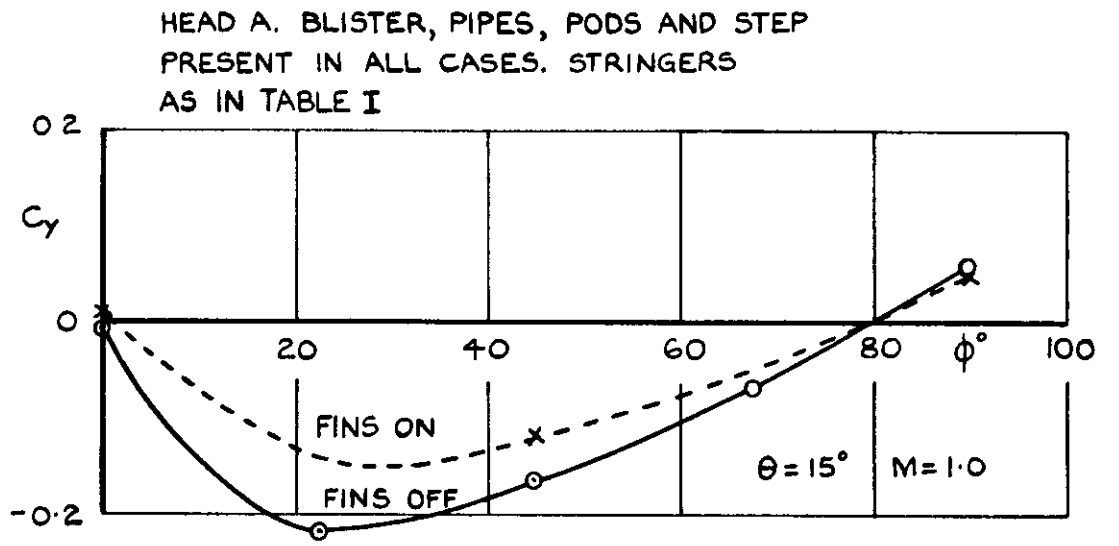

(a) SIDE FORCE

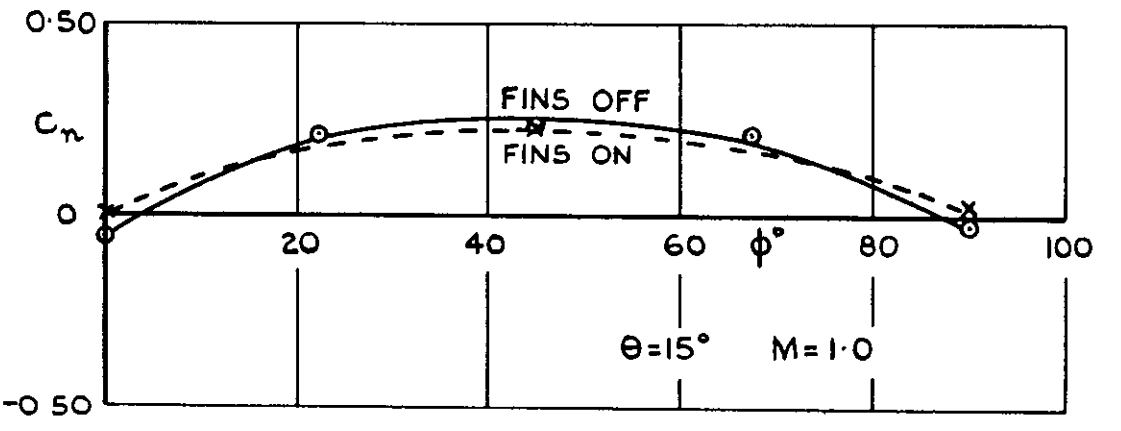

(b) YAWING MOMENT

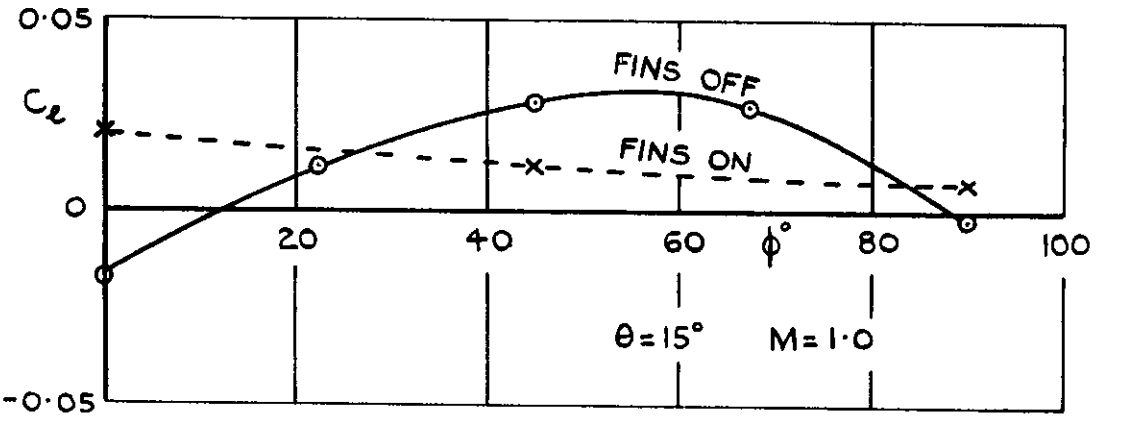

(c) ROLLING MOMENT

FIG.19 (a-c). SIDE FORCE, YAWING MOMENT AND ROLLING MOMENT AT $\theta = 15^\circ$, M = 1·0. (PARA. 5).

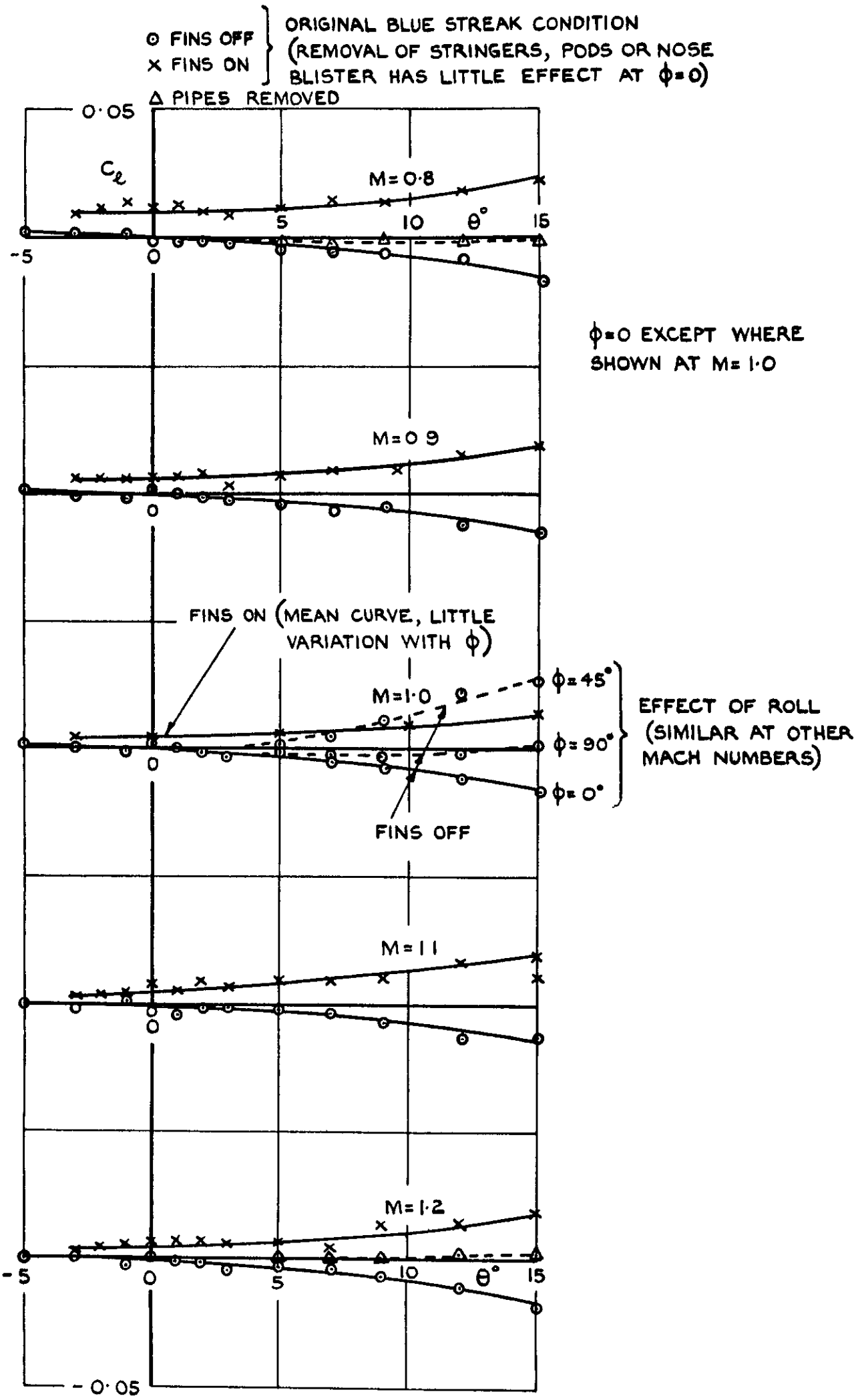

FIG. 20. ROLLING MOMENTS. TYPICAL C_ℓ - θ CURVES (PARA. 5).

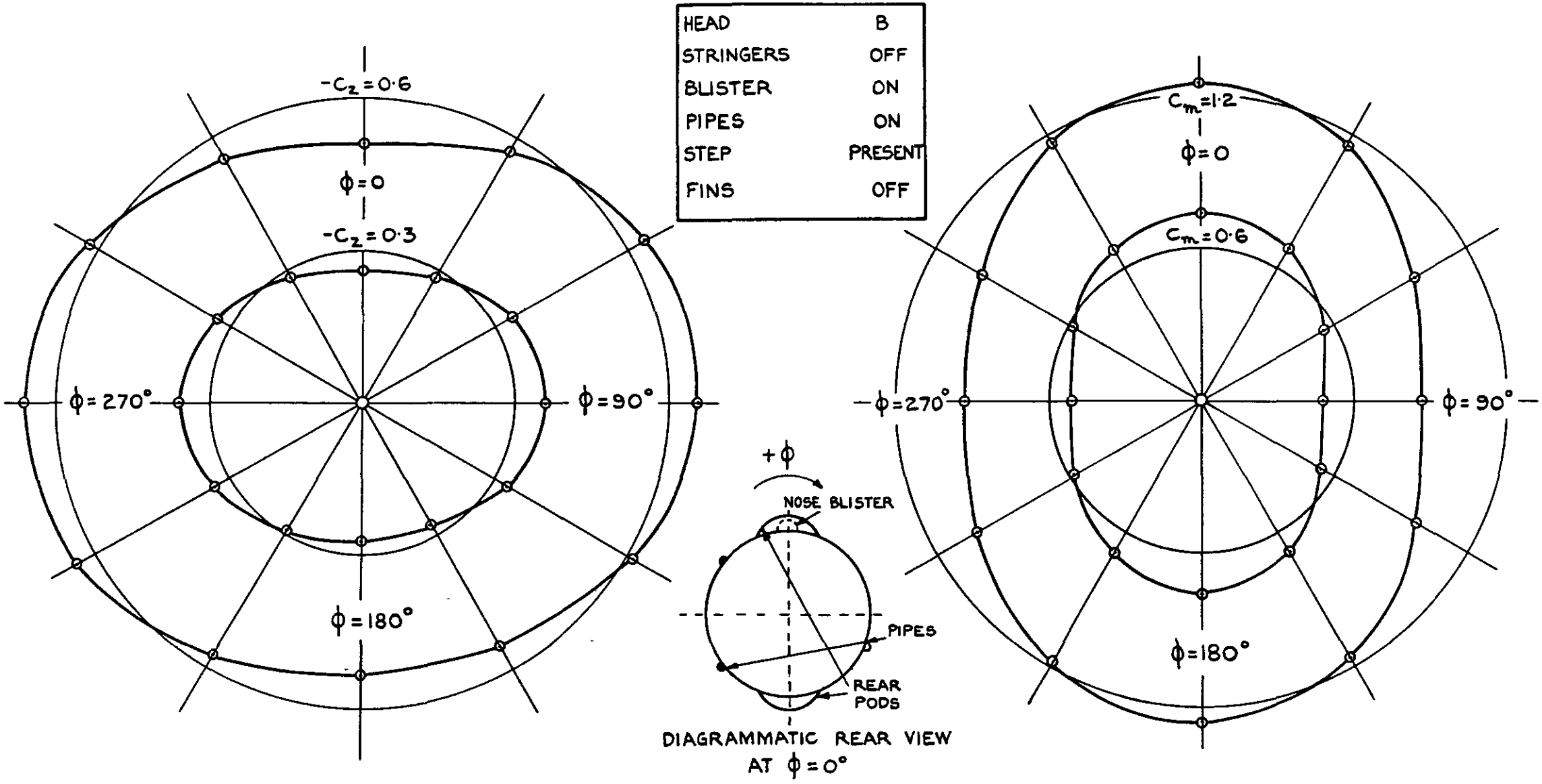

FIG. 21. POLAR DIAGRAMS OF $-C_z$ AND C_m vs. ROLL ANGLE AT $M = 1.19$ (RESULTS FROM 8' × 8' TUNNEL, BEDFORD)

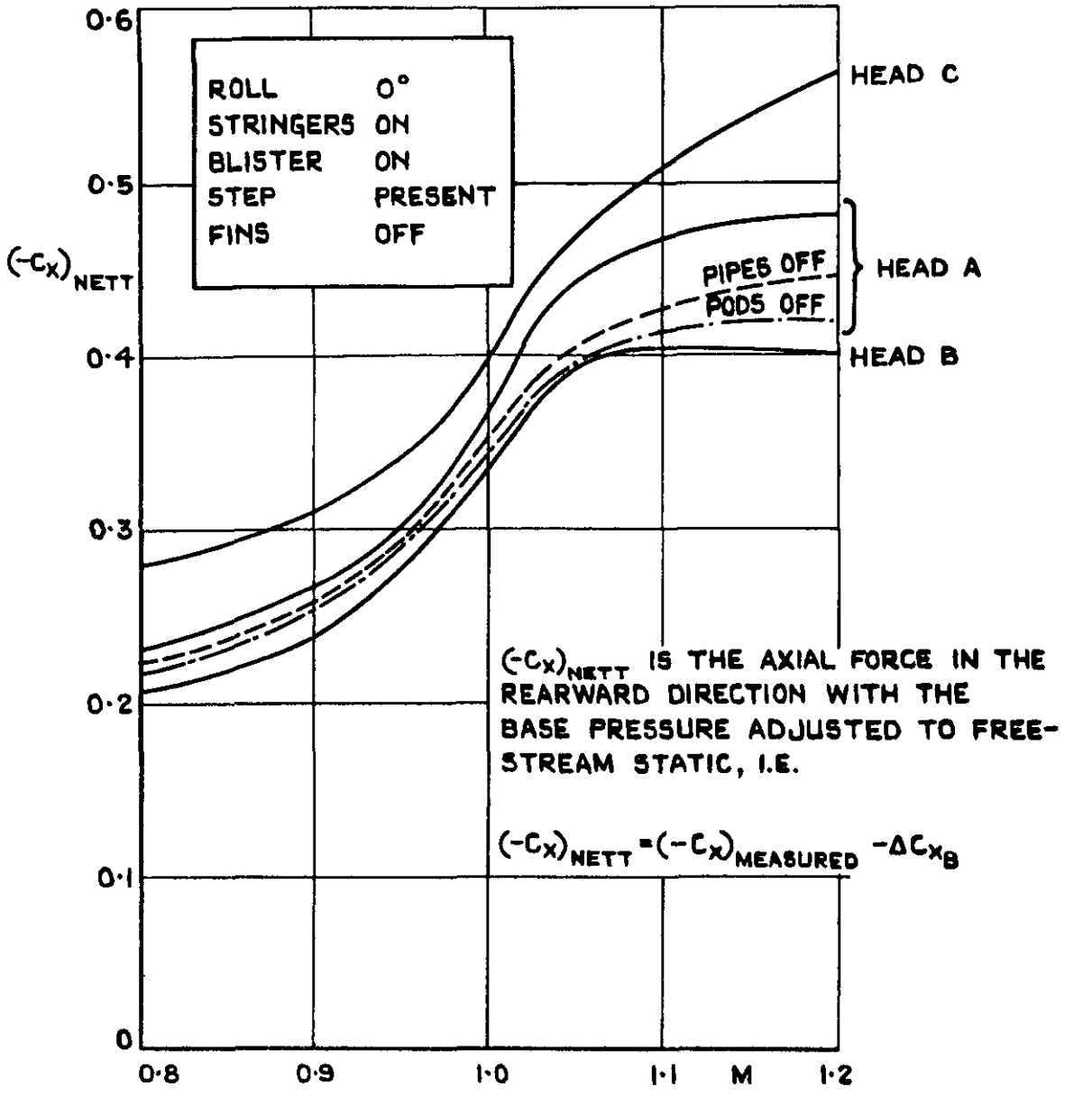

(a) NETT AXIAL FORCE.

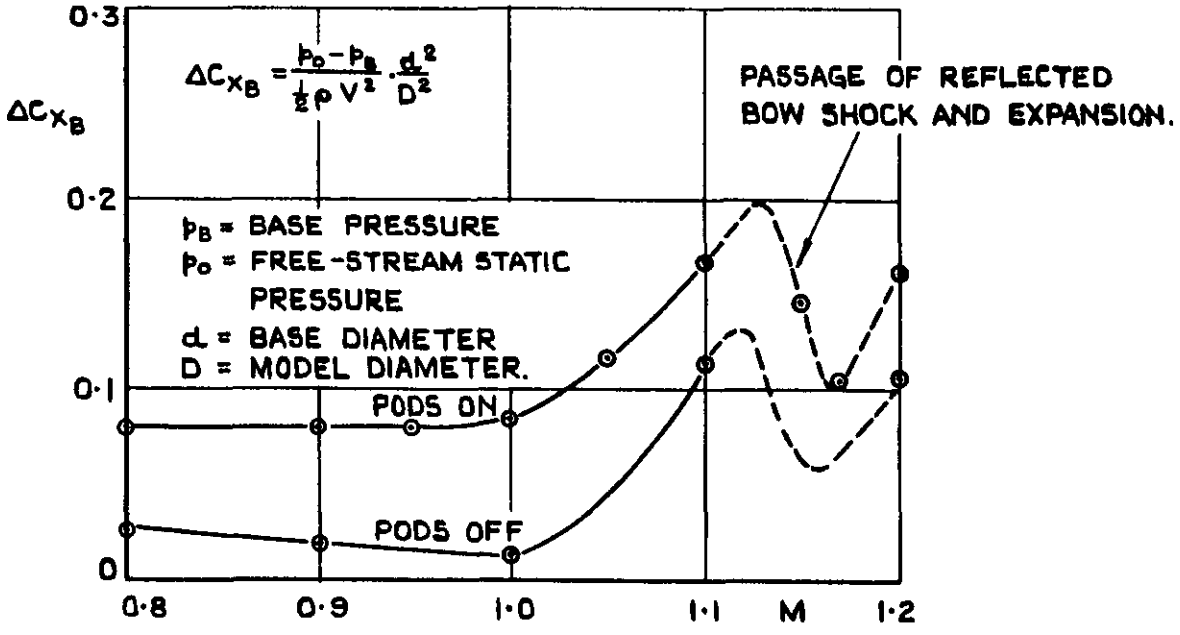

(b) MEAN BASE PRESSURE CORRECTIONS.

FIG. 22 (a & b) AXIAL FORCE vs MACH NUMBER AT ZERO INCIDENCE. (PARA. 6)

A.R.C. C.P. No.735

533.665:
533.6.011.35:
533.6.013.1:
Blue Streak

8 FT X 6 FT TUNNEL TESTS ON A MODEL OF THE DE HAVILLAND "BLUE STREAK" AT MACH NUMBERS OF 0.80 TO 1.25.
Courtney, A.L. April 1959.

Six-component force and moment measurements have been made on a fully representative model of the De Havilland "Blue Streak" at Mach numbers of 0.80 to 1.25, body incidences up to 15° and roll angles up to 90°, to check the static stability characteristics in the transonic speed range.

With fins off the results are free from serious irregularities and the pitching moment is approximately linear with body incidence (θ) about the full-scale centre-of-gravity position. With fins on there is some non-linearity in pitch, particularly at subsonic speeds.

P.T.C.

A.R.C. C.P. No.735

533.665:
533.6.011.35.
533.6.013.1.
Blue Streak

8 FT X 6 FT TUNNEL TESTS ON A MODEL OF THE DE HAVILLAND "BLUE STREAK" AT MACH NUMBERS OF 0.80 TO 1.25.
Courtney, A.L. April 1959.

Six-component force and moment measurements have been made on a fully representative model of the De Havilland "Blue Streak" at Mach numbers of 0.80 to 1.25, body incidences up to 15° and roll angles up to 90°, to check the static stability characteristics in the transonic speed range.

With fins off the results are free from serious irregularities and the pitching moment is approximately linear with body incidence (θ) about the full-scale centre-of-gravity position. With fins on there is some non-linearity in pitch, particularly at subsonic speeds.

P.T.O.

A.R.C. C.P. No.735

533.665.
533.6.011.35:
533.6.013.1:
Blue Streak

8 FT X 6 FT TUNNEL TESTS ON A MODEL OF THE DE HAVILLAND "BLUE STREAK" AT MACH NUMBERS OF 0.80 TO 1.25.
Courtney, A.L. April 1959.

Six-component force and moment measurements have been made on a fully representative model of the De Havilland "Blue Streak" at Mach numbers of 0.80 to 1.25, body incidences up to 15° and roll angles up to 90°, to check the static stability characteristics in the transonic speed range.

With fins off the results are free from serious irregularities and the pitching moment is approximately linear with body incidence (θ) about the full-scale centre-of-gravity position. With fins on there is some non-linearity in pitch, particularly at subsonic speeds.

P.T.O.

The values of $dC_n/d\theta$ at zero roll angle are greater than was expected from simple cone-cylinder tests, the difference amounting to about 2% at M=1 about the full-scale centre-of-gravity position. Component tests show that the increase is entirely attributable to the various external fitments (stringers, fuel pipes, nose blister, rear pods and rear step) all of which increase $dC_n/d\theta$.

The values of $dC_n/d\theta$ at zero roll angle are greater than was expected from simple cone-cylinder tests, the difference amounting to about 2% at M=1 about the full-scale centre-of-gravity position. Component tests show that the increase is entirely attributable to the various external fitments (stringers, fuel pipes, nose blister, rear pods and rear step) all of which increase $dC_n/d\theta$.

The values of $dC_n/d\theta$ at zero roll angle are greater than was expected from simple cone-cylinder tests, the difference amounting to about 2% at M=1 about the full-scale centre-of-gravity position. Component tests show that the increase is entirely attributable to the various external fitments (stringers, fuel pipes, nose blister, rear pods and rear step) all of which increase $dC_n/d\theta$.

Published by
HER MAJESTY'S STATIONERY OFFICE

To be purchased from
York House, Kingsway, London w.c.2
423 Oxford Street, London w.1
13A Castle Street, Edinburgh 2
109 St. Mary Street, Cardiff
39 King Street, Manchester 2
50 Fairfax Street, Bristol 1
35 Smallbrook, Ringway, Birmingham 5
80 Chichester Street, Belfast 1
or through any bookseller

C.P. No. 735

S.O. CODE No. 23-9015-35